© 2014. Published by The Company of Biologists Ltd | Journal of Cell Science (2014) 127, 2433–2447 doi:10.1242/jcs.137281

RESEARCH ARTICLE

An RNAi screen identifies KIF15 as a novel regulator of the endocytic trafficking of integrin

Anastasia Eskova[1], Bettina Knapp[2], Dorota Matelska[1], Susanne Reusing[1], Antti Arjonen[3], Tautvydas Lisauskas[1], Rainer Pepperkok[4], Robert Russell[1], Roland Eils[1,5], Johanna Ivaska[3], Lars Kaderali[2], Holger Erfle[1] and Vytaute Starkuviene[1,*]

ABSTRACT

α2β1 integrin is one of the most important collagen-binding receptors, and it has been implicated in numerous thrombotic and immune diseases. α2β1 integrin is a potent tumour suppressor, and its downregulation is associated with increased metastasis and poor prognosis in breast cancer. Currently, very little is known about the mechanism that regulates the cell-surface expression and trafficking of α2β1 integrin. Here, using a quantitative fluorescence-microscopy-based RNAi assay, we investigated the impact of 386 cytoskeleton-associated or -regulatory genes on α2 integrin endocytosis and found that 122 of these affected the intracellular accumulation of α2 integrin. Of these, 83 were found to be putative regulators of α2 integrin trafficking and/or expression, with no observed effect on the internalization of epidermal growth factor (EGF) or transferrin. Further interrogation and validation of the siRNA screen revealed a role for KIF15, a microtubule-based molecular motor, as a significant inhibitor of the endocytic trafficking of α2 integrin. Our data suggest a novel role for KIF15 in mediating plasma membrane localization of the alternative clathrin adaptor Dab2, thus impinging on pathways that regulate α2 integrin internalization.

KEY WORDS: Integrin, Endocytic trafficking, KIF15, Dab2

INTRODUCTION

Integrins are one of the major cell-surface adhesion receptors, and they are involved in numerous functions, such as cell migration, signal transduction, proliferation, survival and differentiation. Currently, 18 α integrin and 8 β integrin chains are known to be expressed in human cells, forming 24 different heterocomplexes that are specific for diverse ligands (Takada et al., 2007; Humphries et al., 2006; Caswell et al., 2009). The availability and functionality of integrins on the cell surface strongly depends on their biosynthetic trafficking, internalization, recycling and degradation (Margadant et al., 2011).

Newly synthesized integrins are assembled into heterodimers in the endoplasmic reticulum (Heino et al., 1989; Huang et al., 1997), traverse the Golgi complex in the inactive state (Tiwari et al., 2011a) and require binding to TGN38 homolog (also known as TGN46 or TGOLN2) at the trans-Golgi to efficiently reach the plasma membrane (Wang and Howell, 2000). Both ligand-bound (clustered) and non-bound (non-clustered) surface integrins can be internalized (Valdembri et al., 2011; Arjonen et al., 2012), and clathrin-dependent and clathrin-independent pathways have been elucidated for the internalization of different integrins (Caswell et al., 2009). Unlike many other endocytic cargoes, integrin internalization through the clathrin-dependent pathway often requires clathrin-associated sorting proteins [CLASPs; for instance, Dab2, Numb or ARH (also known as LDLRAP1)] (Nishimura and Kaibuchi, 2007; Ezratty et al., 2009, Teckchandani et al., 2009). The majority of the internalized integrins are recycled back to the plasma membrane (Caswell and Norman, 2006) either through Rab11-specific (long-loop) or Rab4-specific (short-loop) pathways (Roberts et al., 2001; Powelka et al., 2004; Arjonen et al., 2012). Ligand-bound integrins can also be directed to lysosomal or non-lysosomal degradation pathways (Arjonen et al., 2012; Valdembri et al., 2009; Rintanen et al., 2012; Lobert et al., 2010; Tiwari et al., 2011b; Dozynkiewicz et al., 2012). Competitive binding of diverse regulators to integrins might promote recycling or intracellular retention (Mai et al., 2011; Böttcher et al., 2012). The exact pathway of integrin trafficking depends not only on the integrin activation state, but also on cell type, composition of the integrin heterodimer, trafficking of other integrins and extracellular stimuli (Caswell and Norman, 2006).

Despite the complexity of trafficking pathways, regulators involved in integrin internalization, recycling or degradation are emerging. Small GTPases of the Rab family (Rab4, Rab5, Rab7, Rab11, Rab21 and Rab25) are crucial regulators of endocytic integrin trafficking (Roberts et al., 2001; Powelka et al., 2004; Arjonen et al., 2012; Pellinen et al., 2006; Caswell et al., 2007), and diverse SNAREs (mediators of membrane fusion) have been described to function in integrin recycling (e.g. the SNAP23–syntaxin-4–VAMP3 complex, syntaxin 3 and syntaxin 6) (Skalski et al., 2010; Veale et al., 2010, Tiwari et al., 2011a; Day et al., 2011). In addition, several molecular motors play a role in integrin trafficking. For instance, actin-based motors, such as myosin 10, regulate integrin-mediated cell adhesion in filopodia (Zhang et al., 2004), and myosin 6 promotes the internalization of ligand-bound α5β1 integrin (Valdembri et al., 2009). The microtubule-based motor KIF1C promotes the delivery of α5β1 integrin from the perinuclear recycling compartment to the trailing edge of migrating cells (Theisen et al., 2012). However, a

[1]BioQuant, University of Heidelberg, 69120 Heidelberg, Germany. [2]Medical Faculty, Institute for Medical Informatics and Biometry (IMB), Technische Universität Dresden, 01307 Dresden, Germany. [3]Centre for Biotechnology, University of Turku, 20520 Turku, Finland. [4]EMBL, Meyerhofstraße 1, 69117 Heidelberg, Germany. [5]Integrative Bioinformatics and Systems Biology, DKFZ, BioQuant and Institute of Pharmacy and Molecular Biotechnology, University of Heidelberg, 69120 Heidelberg, Germany.

*Author for correspondence (vytaute.starkuviene@bioquant.uni-heidelberg.de)

Received 21 June 2013; Accepted 20 February 2014

Journal of Cell Science (2014) 127, 2433–2447 doi:10.1242/jcs.137281

comprehensive characterization of the molecular machinery regulating integrin trafficking is still missing.

β1 integrin is frequently used to investigate integrin trafficking; however, it forms heterodimers with 12 different α chains (Hynes, 2002). As different heterodimers exhibit different trafficking kinetics (Caswell et al., 2009) and might have different molecular requirements (Teckchandani et al., 2009), the analysis of the selected α chain might be more useful to delineate specific molecular mechanisms. α2 integrin interacts only with the β1 integrin subunit (Hynes, 1992), and α2β1 heterodimer is expressed in fibroblasts, keratinocytes, leukocytes, platelets and epithelial and endothelial cells. As one of the most important receptors of collagen (Kramer and Marks, 1989; Hemler et al., 1990; Emsley et al., 2000), α2β1 is crucial for hemostasis, morphogenesis of tubular organs, angiogenesis, platelet aggregation, renewal of the epidermis and wound healing (Chen et al., 2002; Eble, 2005). It is also involved in numerous thrombotic and immune diseases (Eckes et al., 2000; Santoro, 1999; de Fougerolles et al., 2000). Importantly, the expression of α2β1 integrin is strongly reduced in breast cancer, and α2β1 downregulation correlates with increased cell invasion and metastasis and thus with poor prognosis (Zutter et al., 1998; Ramirez et al., 2011). α2β1 integrin also acts as a co-receptor for several pathogens, such as echovirus 1 (EV1), rotavirus and human cytomegalovirus (Bergelson et al., 1992; Londrigan et al., 2003; Feire et al., 2004; Fleming et al., 2011). Binding of EV1 induces clustering of inactive α2β1 and directs virus-bound α2 integrin to a calpain-dependent degradation pathway in multivesicular bodies (Rintanen et al., 2012; Karjalainen et al., 2008; Upla et al., 2004). Binding of α2β1 integrin to collagen might direct the heterodimer to the same degradation pathway (Rintanen et al., 2012). By contrast, little is known about the trafficking route of non-clustered α2β1 integrin, apart from a role for Rab21 binding to the α2 integrin cytoplasmic tail to facilitate endocytosis and a role for binding of the p120 RasGAP (GTPase activating protein; also known as RASA1), which facilitates the recycling of α2β1 integrin to the plasma membrane (Mai et al., 2011).

Here, we used an unbiased quantitative fluorescence-microscopy-based RNAi screen to identify regulators of the endocytic trafficking of α2 integrin. We targeted the expression of 386 chosen proteins that are functionally related to membrane trafficking and the cellular cytoskeleton. Of these, 122 were demonstrated to affect the intracellular accumulation of α2 integrin, and half of these were novel regulators in the context of endocytosis. We chose to characterize in more detail the role of one of the strongest validated inhibitors of α2 integrin trafficking, the molecular motor KIF15. Our data support the novel suggestion that the internalization of α2 integrin is regulated through motor-dependent plasma membrane localization of the alternative clathrin adaptor Dab2.

RESULTS

Endocytic trafficking of endogenous α2 integrin

To define whether α2 integrin undergoes heterodimer-specific endocytic trafficking, we compared the endocytosis of α2 integrin in HeLa cells (chosen for their ease of transfection and high RNAi efficiency) with the previously characterized trafficking of β1 integrin. Cell-surface α2 integrin was antibody-labeled at 4℃ for 1 h and then internalized at 37℃ for varying lengths of time on plastic dishes. In order to quantify the amount of intracellular α2 integrin, the remaining cell-surface integrin–antibody complexes were removed by treating cells with an acidic buffer [see Methods, (Erfle et al., 2011)]. Internalized α2 integrin accumulated efficiently at the juxtanuclear area and cytoplasmic structures (Fig. 1A,D) after 1 h. α2 integrin localized largely to the scattered cytoplasmic structures after a prolonged incubation time of 6 h (Fig. 1A). There was a progressive reduction in the amount of cell-surface α2 integrin (Fig. 1B,E), similar to that measured for β1 integrin in HeLa cells (Teckchandani et al., 2009). By contrast, antibody-clustered α2 integrin (see Methods) accumulated in cytoplasmic punctate structures with hardly any residual plasma membrane localization (Fig. 1C), as reported previously (Rintanen et al., 2012; Karjalainen et al., 2008; Upla et al., 2004).

In order to determine the endocytic route of α2 integrin following internalization, several GFP–Rab-GTPases were overexpressed, and cells were stained for α2 integrin. Similar to results for β1 integrin (Powelka et al., 2004; Arjonen et al., 2012), following 1 h of internalization, >70% of the intracellular α2 integrin colocalized with peripheral structures that were positive for overexpressed Rab5a GTPase (Fig. 2A). Only 10% of the peripheral α2-integrin-containing structures were Rab7a positive (Fig. 2D), suggesting that α2 integrin enters the Rab7a-dependent lysosomal degradation pathway inefficiently. Approximately 70% of the peripheral α2-integrin-containing structures were Rab11b and Rab4a positive (Fig. 2B,C) – a strong indication that α2 integrin enters short- and long-loop recycling pathways. Interestingly, unlike β1 integrin (Powelka et al., 2004), perinuclear localization of α2 integrin was reduced when Rab11b and Rab4a were overexpressed (Fig. 2B,C).

Previous RNAi experiments demonstrated that the endocytosis of β1 integrin occurs through the clathrin-dependent pathway in various cell types (Nishimura and Kaibuchi, 2007; Chao and Kunz, 2009) and by a caveolin-dependent pathway in myofibroblasts (Shi and Sottile, 2008). The latter pathway is also utilized by α2 integrin in ovarian carcinoma cells when the epidermal growth factor receptor is activated (Ning et al., 2007) or upon clustering of α2β1 integrin by antibodies (Upla et al., 2004), suggesting possible cell-type-specific mechanisms. To investigate whether both of these pathways play a role in the endocytic trafficking of α2 integrin in HeLa cells, we depleted the key components of clathrin-dependent and caveolae-dependent pathways [clathrin heavy chain (CLTC), caveolin-1 (CAV1) and dynamin-2 (DNM2)] (Hansen and Nichols, 2009; Doherty and McMahon, 2009). The efficiency of the respective siRNAs was tested by western blotting or immunofluorescence staining, which demonstrated a 50–80% reduction in the levels of the target proteins after 48 h of transfection (supplementary material Fig. S1). Even an incomplete reduction in the expression of CLTC, CAV1 or DNM2 was sufficient to inhibit the intracellular accumulation of α2 integrin by 70–80% (Fig. 1F,G).

Potential regulators of α2 integrin intracellular accumulation identified by RNAi assays

To identify regulators of the intracellular accumulation of α2 integrin, we performed a fluorescence-microscopy-based RNAi screen with 1084 siRNAs targeting 386 genes (supplementary material Table S1). The targeted library (provided by R.P.) was designed to include most mammalian motor proteins, including 44 kinesin heavy chains, 13 dynein subunits (the three major heavy chains and ten cargo-binding light chains) and 37 myosins. In addition, proteins regulating membrane trafficking and/or cytoskeletal dynamics were included based on literature data.

Journal of Cell Science (2014) 127, 2433–2447 doi:10.1242/jcs.137281

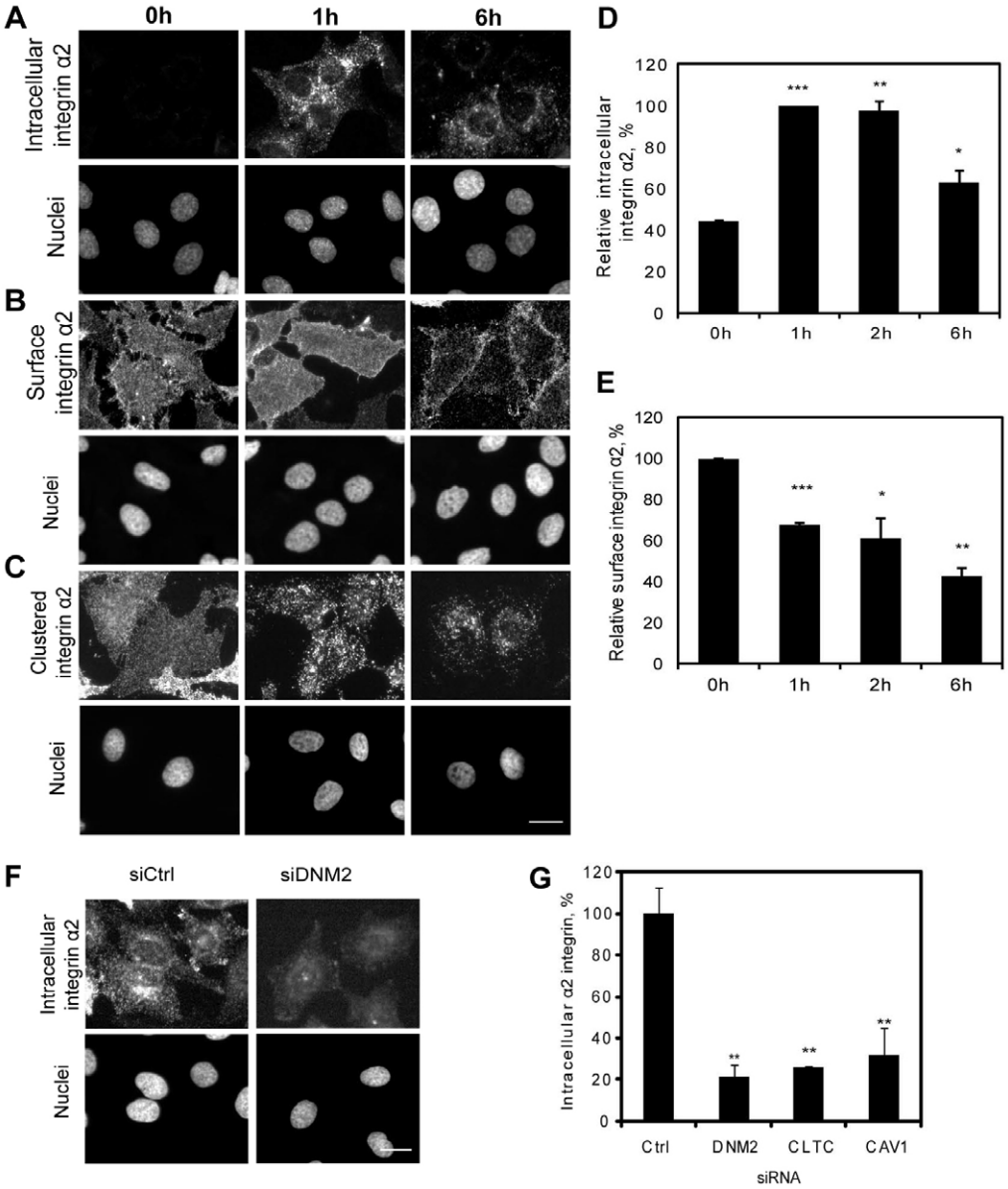

Fig. 1. Endocytic trafficking of endogenous α2 integrin in HeLa cells. Visualization of internalized (A), surface non-clustered (B) and antibody-clustered α2 integrin (C). Quantification of the internalized (D) and cell-surface α2 integrin (E). The amount of the internalized α2 integrin at the 1 h time-point and surface α2 integrin at the 0 h time-point was set to 100% in D and E, respectively. Intracellular accumulation of α2 integrin is clathrin- and caveolin-dependent in HeLa cells (F,G). Ctrl, control. Scale bars: 20 μm. Data show the mean±s.e.m. (three independent experiments); *$P\leq0.05$, **$P\leq0.01$, ***$P\leq0.001$.

This group included 28 small Ras and Rho GTPases, 53 GAPs and 62 GEFs (guanine nucleotide exchange factors) of these GTPases, 41 actin-associated and 14 microtubule-associated proteins, 34 kinases and 9 phosphatases, 5 different β integrin chains, and 23 scaffold and adaptor proteins. For the primary screen, we used Lab-Tek chambers that were pre-spotted with the siRNAs and Lipofectamine [reverse transfection on cell arrays (Erfle et al., 2007)]. These were prepared in one spotting experiment, ensuring a high efficiency and reproducibility of the whole screen (see Methods). We quantified the α2-integrin-specific intracellular fluorescence signal for individual cells after 1 h of internalization, the time-point at which the level of intracellular α2 integrin was the highest in the control sample (Fig. 1D), thereby achieving the best signal-to-noise ratio during the screen. Inspection of the control samples over large cell populations revealed a large variation in the amount of internalized α2 integrin in HeLa cells. As quantification of intracellular α2 integrin in cells with low accumulation efficiency is unreliable, we focused on cells with efficient α2 integrin accumulation. We set a threshold for cells with high levels of intracellular α2 integrin (defined visually during imaging) and subsequently used the empirical cumulative distribution function to define the respective cell population for every experiment (supplementary material Fig. S2), and the Gaussian Mixture Model to automatically separate cell subpopulations (see Methods). Usually, high levels of intracellular α2 integrin were found in 40–50% of HeLa cells transfected with the negative control, and these were used for further analysis to yield high-quality data.

Screen hits were defined according to individual *z*-scores of each siRNA normalized to that of the negative controls (see Methods). Positive *z*-scores indicate increased amounts and negative *z*-scores indicate reduced amounts of intracellular α2 integrin. We considered siRNAs with *z*-scores of greater than 1 or less than −1 (>|1|) as primary hits (supplementary material Table S2). In total, 122 genes were assigned as hits in our screen, of which 115 inhibited and 7 accelerated the intracellular accumulation of α2 integrin (Fig. 3A). Next, we separated the

Journal of Cell Science (2014) 127, 2433–2447 doi:10.1242/jcs.137281

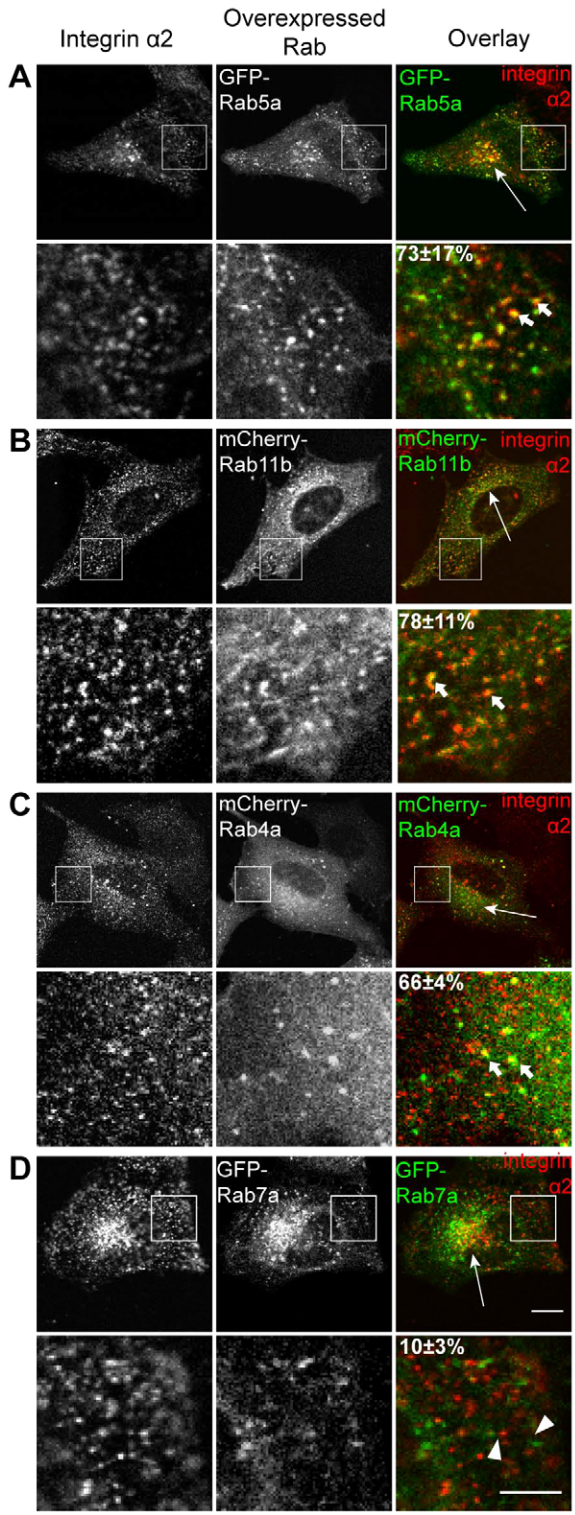

Fig. 2. Colocalization of intracellular α2 integrin with Rab GTPases. Endogenous α2 integrin (red) was colocalized with the overexpressed GFP-tagged Rab5a (A), mCherry-tagged Rab11b (B), GFP-tagged Rab4a (C) and GFP-tagged Rab7a (D) (green) at 1 h after the internalization. The lower row of images shows a higher magnification view of the region indicated by the white box in the upper images. Thick arrows, colocalizing structures; arrowheads, non-colocalizing structures in overlay images; thin arrows, perinuclear localization of the overexpressed Rabs. The figures in the lower right image of each panel show the percentage of α2 integrin that colocalizes with the respective Rab (mean±s.d.). Scale bars: 10 μm (upper row of images), 5 μm (lower row of images).

primary hits into strong (z-score $>|1.5|$) and weak effectors (z-score $<|1.5|$). Downregulation of CLTC and DNM2 produced z-scores of -1.5, corresponding to a strong inhibition of α2 integrin traffic on cell arrays (Fig. 3B). A total of 26 other genes were classified as strong inhibitors, some showing a larger effect that that caused by CLTC and DNM2 downregulation (supplementary material Table S2). For instance, the downregulation of syndecan-4, a protein implicated in the caveolae-dependent internalization of integrins (Bass et al., 2011), led to a strong inhibition (z-score$=-1.78$) of the intracellular accumulation of α2 integrin. The majority of the inhibitors were characterized as weak effectors (90 out of 115). The depletion of CAV1 for 48 h showed a reproducible but weak inhibitory effect (z-score$=-1.14$). In part, this might reflect the level of protein knockdown achieved during the relatively short incubation period with siRNAs (supplementary material Fig. S1). Seven primary hits of the screen were called 'accelerators' (supplementary material Table S2). One of these is ASAP1, a GAP of ARF6 (Randazzo et al., 2007) that has been previously shown to regulate integrin recycling (Onodera et al., 2012). It was scored as a strong accelerator (z-score$=2.26$); this effect was caused by the enhanced accumulation of intracellular α2 integrin, likely due to inhibited recycling.

With the exception of kinases and phosphatases, which were over-represented (19%) among strong effectors in comparison with their representation in the screened library (11%) (supplementary material Tables S1, S2), no significant representation of protein functional class (assigned based on Gene Ontology terms) was observed. While comparing our primary hits to a genome-wide screen for regulators of the endocytosis of transferrin and epidermal growth factor (EGF) (Collinet et al., 2010), we found that 39 out of 122 of our hits (32%) were reported as regulators of either transferrin or EGF endocytosis, and 83 primary hits from our screen appeared to be specific only to the intracellular accumulation of α2 integrin (Fig. 3C).

As endocytic trafficking of integrins is fundamental for the regulation of focal adhesion dynamics and cell migration (Morgan et al., 2013; Chao and Kunz, 2009; Caswell and Norman, 2008), we compared the results of our screen with those of two relevant published RNAi screens (Winograd-Katz et al., 2009; Simpson et al., 2008) (Fig. 3C). In addition, 161 genes from our experiments were also screened to identify regulators of focal adhesions and cell migration (Winograd-Katz et al., 2009; Simpson et al., 2008). We identified 24 out of 161 genes (15%) that were primary hits for both α2 integrin intracellular accumulation and focal adhesion formation, including the phosphatidylinositol phosphatase PTEN (Mise-Omata et al., 2005). We found that 9 out of 161 genes (5.5%) were positive both in our assay and in a previously published cell migration assay (Simpson et al., 2008).

We observed a fairly large overlap between our primary hits and the components of integrin-primed complexes. Our screen included 45 out of 467 identified non-redundant components of α5β1 and α4β1 integrins (Humphries et al., 2009) and, of these, 19 were assigned as potential regulators of the intracellular accumulation of α2 integrin [e.g. the molecular motors KIF2C and cytoplasmic dynein 1 heavy chain 1 (DYNC1H1)]. A recent search for β1-integrin-interacting proteins (Böttcher et al., 2012)

Journal of Cell Science (2014) 127, 2433–2447 doi:10.1242/jcs.137281

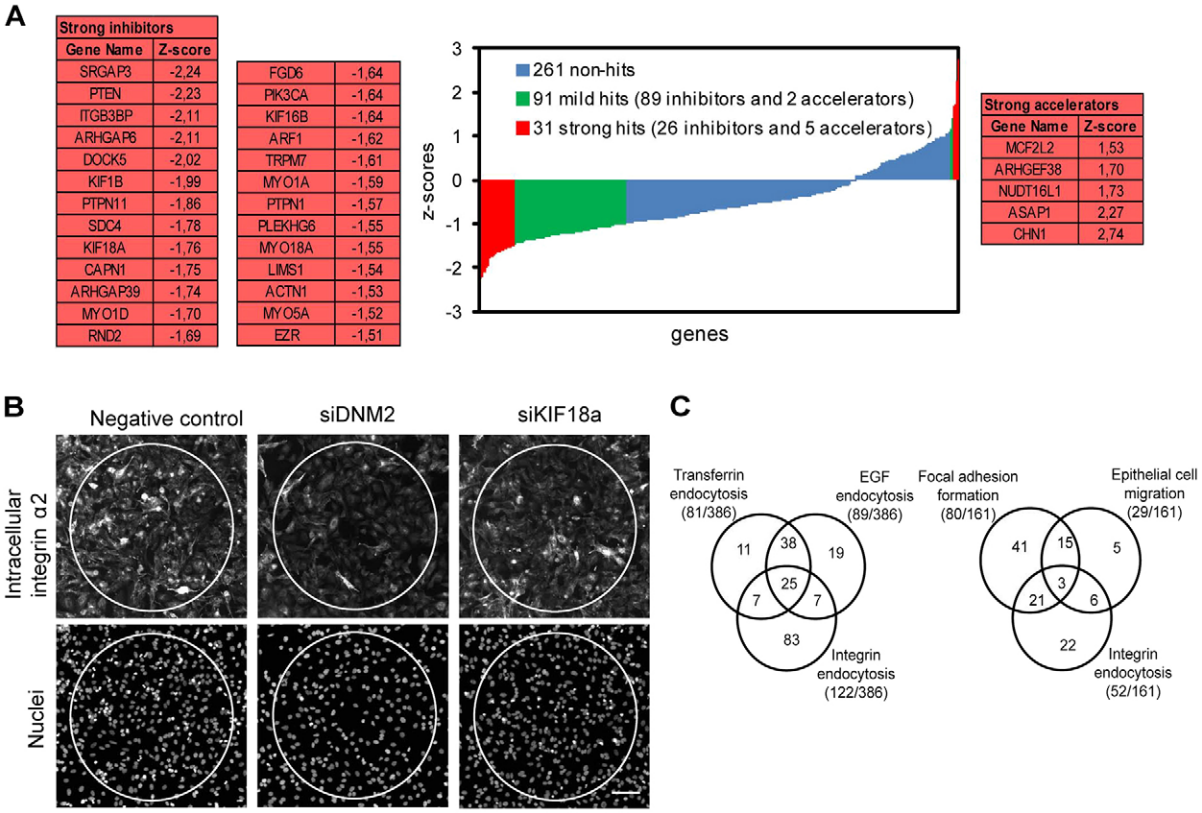

Fig. 3. A fluorescence-microscopy-based screen identifies potential regulators of endocytic trafficking of α2 integrin. (A) Distribution of the *z*-scores of 386 tested genes in the primary screen (the *z*-score of the most effective siRNA is shown for every gene, *z*-scores of other siRNAs are shown in the supplementary material Table S2). Strong hits (*z*-scores >|1.5|) are listed and shown in red; weak hits (*z*-score <|1.5|) are shown in green and non-effectors (*z*-score <|1|) are shown in blue. (B) Examples of intracellular accumulation of α2-integrin-specific fluorescence on cell arrays. White circles indicate spot boundaries within which α2-integrin-specific fluorescence was measured. Scale bar: 100 µm. (C) Comparison of potential regulators of the intracellular accumulation of α2 integrin with the regulators of transferrin and EGF endocytosis (left), and regulators of focal adhesion formation and epithelial cell migration (right).

yielded 96 proteins, of which 11 were tested in our study, and four of these were assigned as primary hits (supplementary material Table S2). These included the integrin-activating protein kindlin-1 (also known as FERMT1) (Moser et al., 2009), LIMS1 [an adaptor protein that connects integrins, small GTPases and EGF signaling pathways (Tu et al., 1999)] and RALBP1 [a GAP of Rac1 and Cdc42 (Matsubara et al., 1997)]. Our screen revealed a number of potential novel regulators of α2 integrin trafficking; for example, KIF18A, a key component of chromosome congression in mitosis (Mayr et al., 2007), strongly inhibited the intracellular accumulation of α2 integrin when downregulated (Fig. 3B).

Validation of potential regulators of α2 integrin intracellular accumulation

To validate the potential regulators of α2 integrin trafficking that were identified in the siRNA screen described above, we selected a fifth of the primary hits (23 proteins). One of the selected groups included the kinesins, as very little is known about the role of these molecular motors in integrin trafficking, and essentially all kinesins were tested in the primary screen (supplementary material Table S1) (Hirokawa et al., 2009). Validation assays were performed in non-coated multi-well plates under direct transfection conditions. Intracellular accumulation was considered as inhibited when the pool of intracellular α2 integrin was reduced by >40% compared with that of the negative control. We scored potential hits as validated when at least two out of four siRNAs showed the same effect as in the primary screening (supplementary material Table S4). From the nine primary hit kinesins that are expressed in HeLa cells (supplementary material Table S3), three, namely KIF15, KIF18A and KIF23 were validated as effectors of α2 integrin intracellular accumulation (Table 1). As kinesins are important trafficking regulators, we extended our investigation beyond the nine kinesins identified as primary hits in our screen. We re-tested 13 more traffic-related kinesins that were non-hits in the primary screen (supplementary material Tables S3, S4) and demonstrated that only KIF13A, a recycling regulator in melanocytes (Delevoye et al., 2009), affected the intracellular accumulation of α2 integrin in the validation experiments. As this result was obtained only with the additional siRNAs, but not with the ones used for the primary screen, we did not include KIF13A in the list of validated hits.

Next, we tested whether decreased levels of intracellular α2 integrin are a direct consequence of inhibited trafficking or reduced protein expression. To do this, we measured the total amounts of α2 integrin following downregulation of the validated kinesins (Table 1). Expression levels of α2 integrin were not affected when KIF15, KIF18A and KIF23 were downregulated (supplementary material Fig. S3). As these kinesins were shown

Journal of Cell Science (2014) 127, 2433–2447 doi:10.1242/jcs.137281

Table 1. Validated regulators of the intracellular accumulation of α2 integrin

Gene name	Intracellular α2 integrin (%)	Total α2 integrin (%)	Cell count (%)
Negative control	100	100	100
DNM2	27.20±6.63	82.45±13.77	98.56±6.88
ARF1	49.17±7.43	99.11±17.67	99.16±37.85
ABL2	52.78±9.94	56.84±4.49	72.05±18.60
ARHGAP6	42.03±6.35	43.14±4.33	75.59±7.24
ITGB1	7.38±3.40	54.12±7.10	99.93±17.32
KIF15	27.80±4.45	96.50±2.30	106.44±7.75
KIF18A	51.12±9.54	97.64±16.74	98.64±31.44
KIF23	25.40±6.36	92.69±33.23	49.11±22.74
Myo1A	36.43±17.79	64.72±4.04	126.42±46.71
NF2	35.59±3.10	95.89±13.64	85.77±3.19
PTPN11	39.11±5.19	76.83±3.72	66.07±28.10

Validated regulators that inhibit the intracellular accumulation of α2 integrin without changing α2 integrin expression are shown in bold. Intracellular and total levels of α2 integrin represent the mean±s.e.m. of α2-integrin-specific fluorescence derived from cells showing efficient endocytosis and all cells, respectively.

to play a role in mitosis (Mayr et al., 2007; Tanenbaum et al., 2009; Zhu et al., 2005b), we calculated the number of cells remaining after 48 h of transfection with the respective siRNAs. Downregulation of KIF23 expression reduced the number of cells by nearly twofold, whereas downregulation of KIF15 and KIF18A did not induce a significant change in the number of cells (Table 1).

To get a better overview of the specificity of our screen we retested 14 additional primary hits belonging to diverse functional groups. To do this, we chose the molecules that were scored as effectors with multiple siRNAs in the primary screen (supplementary material Table S2). RNAi-mediated inhibition of seven of these proteins strongly reduced levels of intracellular α2 integrin in the validation assays (Table 1; supplementary material Table S4). Five of these were also classified as strong inhibitors in the primary screen (ARF1, ABL2, ARHGAP6, Myo1A and PTPN11). Suppressing the expression of two of these proteins (ARF1 and NF2) did not alter the expression levels of α2 integrin, suggesting a role for these proteins in α2 integrin trafficking. ITGB1 and Myo1A reduced α2 integrin expression when downregulated; however, these proteins might play a role in α2 integrin trafficking, as inhibition of the intracellular accumulation of α2 integrin was more pronounced than the effects seen on α2 integrin expression (Table 1). By contrast, the observed effect on intracellular α2 integrin levels upon ABL2 and ARHGAP6 downregulation was largely due to the reduction in total α2 integrin expression. Downregulation of only PTPN1 significantly reduced cell numbers (by nearly 35%).

In summary, we could recapitulate the results of the primary screen for 10 out of the 23 hits (43%). For nearly half of the targets this effect could be attributed to changes in the accumulation of intracellular α2 integrin, whereas the other hits primarily affected the expression level of α2 integrin.

Internalization of α2 integrin is KIF15 dependent

To gain more detailed insight regarding what appeared to be novel regulators revealed by our targeted screen, we focused on KIF15, as no trafficking-related function has been described for KIF15 so far. RNAi of KIF15 for 48 h resulted in a 70% reduction in KIF15 protein levels (supplementary material Fig. S4A,C) and led to a strong inhibition of the intracellular accumulation of α2 integrin without a significant change in α2 integrin expression level and cell numbers (Table 1; supplementary material Fig. S3A,B). Consistent with a decrease in α2 integrin intracellular levels, suppression of KIF15 expression led to a concomitant increase in cell-surface α2 integrin (supplementary material Fig. S3C). Moreover, moderate expression of ectopic GFP-tagged KIF15 (Tanenbaum et al., 2009) (the expression level of which was 3.3-fold that of the endogenous protein) (supplementary material Fig. S4B,D) induced an increase in the amount of intracellular α2 integrin by ~40% (Fig. 4A,B), with α2 integrin accumulating at the perinuclear region after 1 h of internalization. Overexpression of GFP alone under these conditions had no apparent influence. GFP-tagged KIF15 mostly localized to the cytoplasm (Fig. 4A), with occasional localization to the plasma membrane, punctate cytoplasmic structures and microtubules. As GFP-tagged murine KIF15 is resistant to human siRNAs, we performed rescue experiments, which showed that the siRNA-mediated inhibitory effect of KIF15 on the intracellular accumulation of α2 integrin was lessened by 30% (Fig. 4B) following overexpression of GFP-tagged KIF15. The role of KIF15 in α2 integrin endocytic trafficking was further confirmed by using biotin-capture enzyme-linked immunosorbent assays (ELISAs) (Margadant et al., 2012; Roberts et al., 2001) (Fig. 4C). In addition, endocytosis of β1 integrin was also inhibited, as measured by a ratiometric quenching antibody-based assay (Arjonen et al., 2012) (Fig. 4D). Both assays revealed a lower inhibition rate of integrin trafficking (around 25%) when KIF15 was downregulated as compared with the microscopy-based assay (Table 1). This might be attributed to the difference in quantifying the whole cell population in these assays versus a defined subpopulation of cells for the microscopy-based assay (see Methods). No significant changes in actin and microtubule cytoskeleton were observed following KIF15 downregulation (Fig. 4E,F). Taken together, depletion of KIF15 inhibited the intracellular accumulation of α2 integrin in different types of cells (supplementary material Fig. S3D).

Next, we analyzed at which stage the intracellular accumulation of α2 integrin was affected when KIF15 was depleted. In cells transfected with the negative control, α2 integrin gradually accumulated within the cells, whereas downregulation of KIF15 strongly inhibited the intracellular accumulation of α2 integrin throughout the assay (5–60 min) (Fig. 5A,D). We then tested the effect of KIF15 downregulation on the trafficking of EGF that is degraded in lysosomes (Carpenter and Cohen, 1976) and transferrin that is recycled to the plasma membrane (Dickson et al., 1983). In agreement with

Journal of Cell Science (2014) 127, 2433–2447 doi:10.1242/jcs.137281

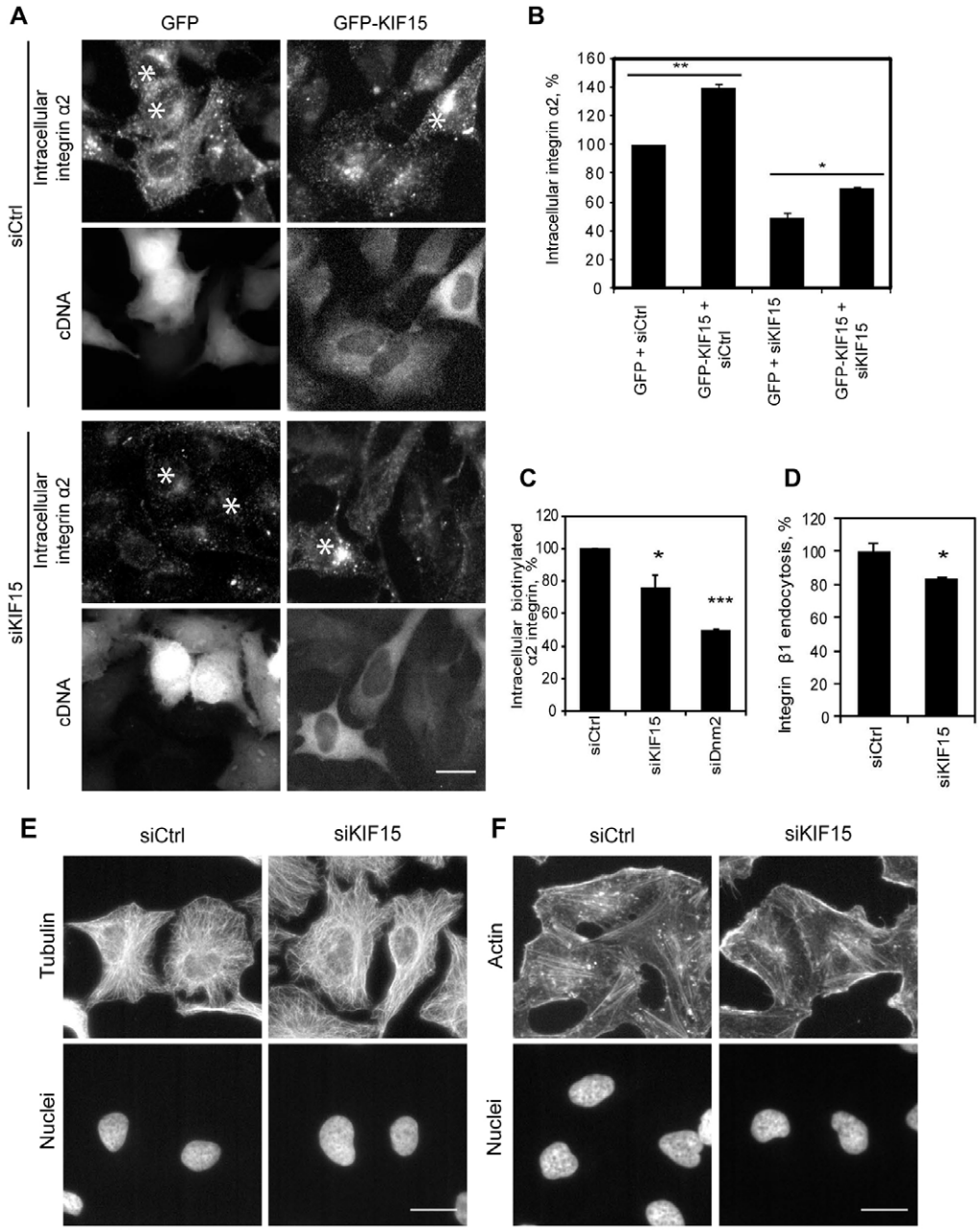

Fig. 4. Validation of the role of KIF15 in the endocytic trafficking of α2 integrin. (A) Depletion of KIF15 by RNAi prevents the appearance of intracellular α2 integrin, and this effect is lessened by the overexpression of GFP-tagged KIF15, but not GFP. Asterisks, cells expressing high levels of GFP and GFP-tagged KIF15. Ctrl, control. (B) Quantification of the rescue of α2 integrin trafficking inhibition. (C,D) Biotin-capture ELISA-based assay (C) and quenching-antibody-based assay (D) show that the intracellular accumulation of α2 integrin and β1 integrin, respectively, is inhibited when KIF15 is downregulated. Data show the mean±s.e.m.; *$P\leq0.05$, **$P\leq0.01$, ***$P\leq0.001$. Downregulation of KIF15 does not affect microtubules (E) or actin (F). Scale bars: 20 μm.

previous results (Collinet et al., 2010), downregulation of KIF15 had no influence on the internalization of either EGF or transferrin cargoes at early time-points (Fig. 5B,C,E,F). However, later steps of transferrin trafficking were significantly affected by KIF15 downregulation (Fig. 5E), with the cargo accumulating in the perinuclear region (Fig. 5B). Presumably, the observed effect is due to inhibited recycling of transferrin to the plasma membrane. By contrast, EGF endocytic trafficking was not influenced by KIF15 downregulation at any time-point (Fig. 5C,F).

KIF15 is required for cell-surface localization of Dab2

We sought to further investigate the integrin-related trafficking function of KIF15. It has been shown that several CLASPs (alternative clathrin adaptors) are required for integrin internalization (Nishimura and Kaibuchi, 2007; Teckchandani et al., 2009). By contrast, internalization of the transferrin receptor is not dependent upon CLASPs such as Dab2 (Teckchandani et al., 2009; Teckchandani et al., 2012; Maurer and Cooper, 2006; Keyel et al., 2006). In our experiments, RNAi of Dab2, ARH and Numb for 48 h caused >80% reduction in the level of the respective transcripts (Fig. 6D), and the same conditions were used to assess the potential role of these CLASPs in α2 integrin trafficking. The strongest inhibition of α2 integrin endocytosis was obtained by depletion of Dab2 (Fig. 6A–C). RNAi of ARH had a weaker effect, whereas suppression of Numb showed no significant inhibition. Our data agree well with previous studies (Chao and Kunz, 2009; Teckchandani et al., 2012) showing that Dab2 strongly inhibits the internalization of β1 integrin when downregulated. Furthermore, surface levels of integrins β1 and α2 increase in Dab2-deficient HeLa cells (Teckchandani et al., 2009).

Journal of Cell Science (2014) 127, 2433–2447 doi:10.1242/jcs.137281

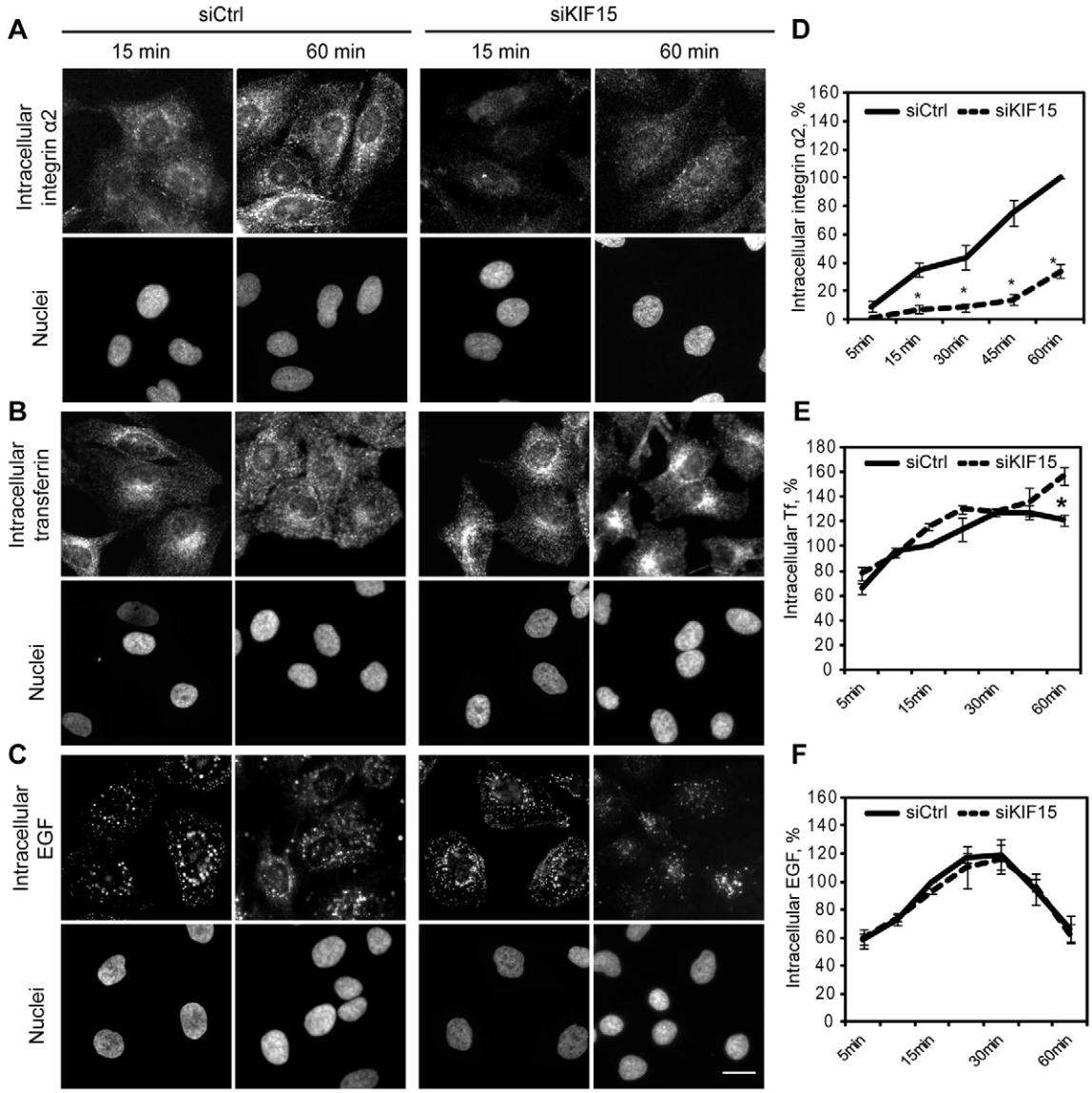

Fig. 5. KIF15 is specifically required for the internalization of α2 integrin. Downregulation of KIF15 inhibits the internalization of α2 integrin (A), but the internalization of transferrin (B) and EGF (C) is not affected. By contrast, the recycling of transferrin to the plasma membrane is strongly inhibited (B). Scale bar: 20 μm. Quantification of the endocytic trafficking of α2 integrin (D), transferrin (Tf) (E) and EGF (F). Lines represent the averaged intracellular intensities of each cargo, normalized to negative controls after 60 min of internalization of α2 integrin and 15 min of internalization of transferrin and EGF. Ctrl, control. Error bars indicate s.e.m. (three independent experiments). $^{*}P \leq 0.05$.

We next tested whether Dab2 is functionally dependent upon KIF15. In agreement with previous studies (Teckchandani et al., 2009; Chetrit et al., 2011), Dab2 localized to punctate structures that were found both on the plasma membrane and intracellularly in HeLa cells imaged in total internal reflection fluorescence (TIRF) and epifluorescence modes (Fig. 7A). Downregulation of KIF15 induced a >40% loss of the cell-surface-associated Dab2 (Fig. 7C,D), with a large fraction of Dab2-specific structures being redistributed from the plasma membrane to the cytoplasm (Fig. 7B). The total level of Dab2 in cells was not changed significantly under these conditions (Fig. 7B; supplementary material Fig. S4F). The role of KIF15 in Dab2 distribution was further demonstrated by a 2.7-fold more frequent accumulation of intracellular Dab2 in the perinuclear region following the depletion of KIF15 (Fig. 7D), indicating that KIF15 might play a role in recycling pathways. Surprisingly, no significant colocalization between Dab2 and α2 integrin was obtained at 37℃, regardless of KIF15 expression levels. It is possible that trapping of integrin at low temperatures is required, as demonstrated for β1 integrin (Teckchandani et al., 2009). Taken together, our data suggest that KIF15 mediates the cell-surface localization of Dab2 that, in turn, might regulate the internalization of α2 integrin.

DISCUSSION

Defective endocytosis of integrins leads to numerous alterations in signaling, cell cycle progression, cell–extracellular-matrix interactions and the cytoskeleton, crucial processes of cancer initiation, progression and metastasis (Mosesson et al., 2008; Shin et al., 2012; Desgrosellier and Cheresh, 2010). Integrin α2β1 is

Journal of Cell Science (2014) 127, 2433–2447 doi:10.1242/jcs.137281

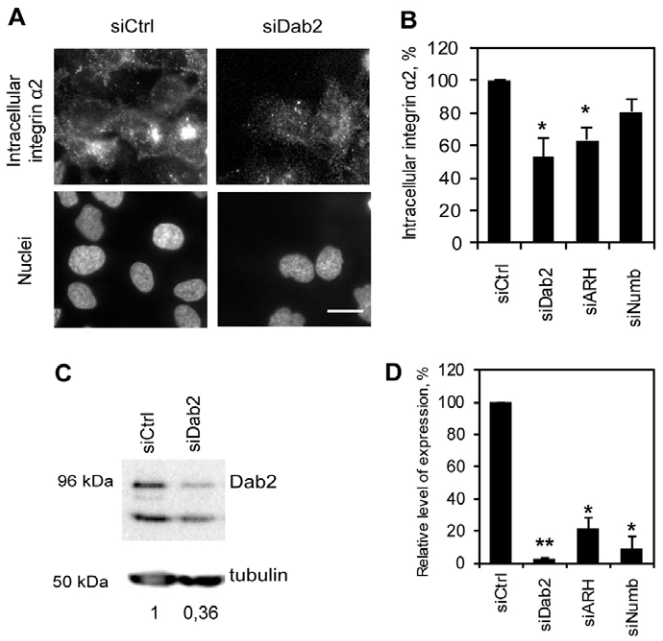

Fig. 6. Depletion of CLASPs inhibits the intracellular accumulation of α2 integrin. Downregulation of Dab2 and ARH prevents the intracellular accumulation of α2 integrin (A,B), whereas downregulation of Numb has no effect (B). (C) The downregulation efficiency of Dab2, as shown by western blotting. (D) The downregulation of mRNAs encoding Dab2, Numb and ARH as shown by quantitative RT-PCR. Ctrl, control. Scale bar: 20 μm. Data show the mean±s.d.; $^{*}P\leq0.05$, $^{**}P\leq0.01$.

known as a potent suppressor of breast cancer metastasis (Ramirez et al., 2011); however, little is known about the endocytic trafficking of this heterodimer. We show here that endogenous α2 integrin in HeLa cells passes through a Rab5-specific compartment and is potentially recycled to the plasma membrane by Rab4- and Rab11- specific structures (Fig. 2). Interestingly, depletion of not only clathrin but also caveolin-1 induced a comparably strong inhibition of the intracellular accumulation of α2 integrin (Fig. 1F,G). Both pathways might act in parallel; however, RNAi-based perturbation of individual pathways could invoke broad cellular responses (Doherty and McMahon, 2009). Alternatively, our data opens an intriguing possibility that clathrin- and caveolin-dependent mechanisms might act in a sequential manner. Nevertheless, the endocytic route of unbound α2 integrin differs strongly from the calpain-dependent degradation pathway taken by the antibody-clustered α2 integrin (Rintanen et al., 2012). With the goal of defining a substantial proportion of the proteins affecting the cell-surface expression of α2 integrin, we performed a fluorescent microscopy-based RNAi screen (Fig. 3).

In total, 386 genes associated with membrane traffic and cytoskeletal organization, and encompassing most mammalian motor proteins, were tested (supplementary material Table S1), with 122 molecules scored as potential regulators of the intracellular accumulation of α2 integrin (Fig. 3A; supplementary material Table S2). Predominantly, a reduction in α2 integrin intracellular accumulation was recorded (for 115 potential regulators), and only seven molecules increased the intracellular accumulation of α2 integrin when downregulated. In the subsequent validation experiments, some of the inhibitors were shown to reduce the overall expression of α2 integrin in cells; however, specific inhibitors of trafficking, such as KIF15, were also identified. We found that 83 primary hits of our screen might be specific to the intracellular accumulation of α2 integrin, as they were not identified as regulators of transferrin or EGF endocytosis [Fig. 3C; (Collinet et al., 2010)]. Possibly, the different outputs of the screens reflect differences between data acquisition (wide field versus confocal microscopy), read-out (monoparametric versus multiparametric), data normalization procedures and testing different siRNA libraries. By contrast, both screens were performed in HeLa cells and, unsurprisingly, there was a fairly large overlap of our hits (39 out of 122) with the regulators of transferrin and EGF endocytosis [Fig. 3C; (Collinet et al., 2010)]. Interestingly, nearly half of the interacting partners of β1 integrin (Böttcher et al., 2012) present in our library were also effectors of α2 integrin trafficking (supplementary material Table S2), but little overlap could be found with the proteomics analysis of interacting partners of the overexpressed and tagged α2 integrin in HT1080 cells (Uematsu et al., 2012). Potentially, this is due to a different cellular context and/or expression levels of integrin. Surprisingly, 24 out of 122 potential regulators of α2 integrin trafficking are known as potential regulators of focal adhesion formation [Fig. 3C; (Winograd-Katz et al., 2009)], indicating a functional crosstalk between the trafficking of unbound and ligand-bound integrins.

For data validation, we chose several subsets of the primary hits. One subset contained 14 functionally heterogeneous molecules that were recorded as hits by multiple siRNAs in the primary screen (supplementary material Table S2) and seven of them were validated (Table 1). Curiously, only two of them – NF2 (also known as Merlin) and a small GTPase, ARF1 – predominantly influenced the intracellular accumulation of α2 integrin, whereas others appeared to influence primarily a2 integrin expression levels. ARF1 is a key component of the COPI coatomer complex and one of the most important trafficking regulators (Donaldson and Klausner, 1994; D'Souza-Schorey and Chavrier, 2006; Volpicelli-Daley et al., 2005). Potentially, ARF1 inhibits α2 integrin trafficking by regulating its recycling to the plasma membrane as was demonstrated for α5 integrin (Krndija et al., 2012); however, other functions of ARF1 cannot be excluded. NF2/Merlin might act indirectly by providing a linkage between membrane-associated proteins and the actin cytoskeleton, thus regulating membrane organization (Li et al., 2012; McClatchey and Giovannini, 2005). By contrast, the Drosophila ortholog of NF2/Merlin localizes to the endocytic compartment in S2 cells (McCartney and Fehon, 1996), and it was reported that NF2/Merlin binds to β1 integrin in Schwann cells (Obremski et al., 1998), suggesting a more direct role for these proteins in integrin traffic.

Another subset of potential regulators chosen for validation analysis were kinesins, microtubule-based molecular motors. Systematic analysis of kinesins has already been performed in the context of cell cycle regulation (Tanenbaum et al., 2009; Goshima and Vale, 2003; Neumann et al., 2010; Zhu et al., 2005a) and membrane trafficking (Collinet et al., 2010; Paul et al., 2011; Simpson et al., 2012), but information about their roles specifically in integrin trafficking is missing. We observed no effect on α2 integrin trafficking when downregulating 13 kinesins that had no effect in the primary screen (supplementary material Tables S2, S4), indicating high fidelity of our assays. Of the nine kinesins recorded as primary hits, three (KIF15, KIF18A and KIF23) strongly inhibited the endocytic trafficking of α2 integrin (Table 1). As expected, the validation rate of kinesins

Journal of Cell Science (2014) 127, 2433–2447 doi:10.1242/jcs.137281

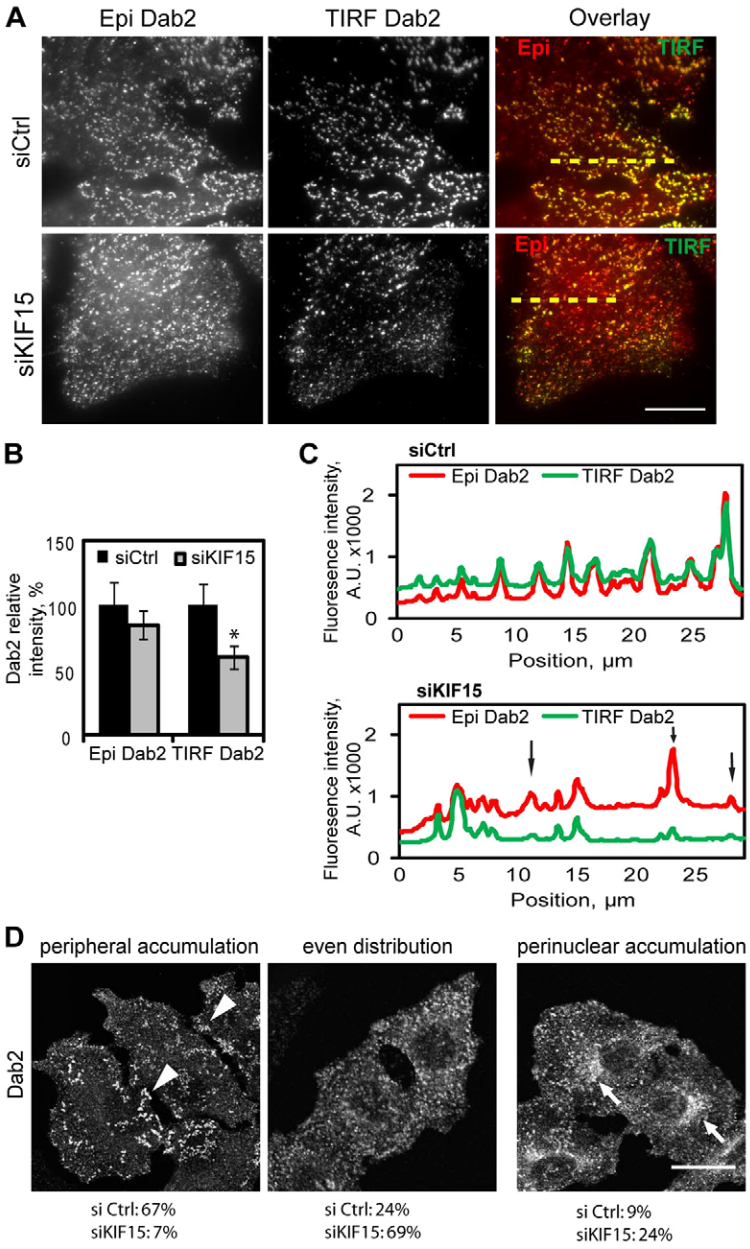

Fig. 7. KIF15 downregulation redistributes Dab2 from the plasma membrane. (A) Downregulation of KIF15 displaces Dab2 associated with the plasma membrane (TIRF imaging mode) to the intracellular space (epifluorescence imaging mode, Epi). Epifluorescence and TIRF images are overlaid; dashed line, the position that was used for fluorescence intensity profile plotting. (B) Quantification of Dab2-specific fluorescent intensities imaged in Epi and TIRF modes. Data show the mean±s.e.m; $n=15$; $^*P\leq0.05$. (C) Fluorescence intensity profile plot, showing Dab2-specific structures by TIRF and Epi modes. Black arrows, Dab2-specific structures that are redistributed from the plasma membrane. Position (*x*-axis) indicates the distance from the left end of the dashed line in A. (D) KIF15 downregulation leads to loss of peripheral Dab2 (arrowheads) and appearance of perinuclear Dab2 (white arrows), as visualized by confocal microscopy. 160 cells transfected with the negative control (Ctrl) and 200 cells transfected with siRNAs targeting KIF15 were analyzed. Scale bars: 20 µm.

was lower than that of the regulators targeted with the multiple siRNAs. However, the validated ones are most likely actual trafficking regulators as none of them changed the expression level of α2 integrin. Indeed, KIF15 and KIF23 have been identified as potential regulators of the biosynthetic trafficking of ts-O45-G (a temperature-sensitive mutant of vesicular stomatitis virus) (Simpson et al., 2012).

In this study, we have focused on KIF15, one of the strongest validated effectors of intracellular accumulation of α2 integrin. Downregulation of KIF15 inhibited intracellular accumulation of α2 and β1 integrins, as shown by several complementing approaches (Table 1; Fig. 4C,D; Fig. 5A,D) without having any effect on cell numbers. The latter observation is in agreement with the notion that KIF15 can be replaced by Eg5 (also known as KIF11) (Tanenbaum et al., 2009; Florian and Mayer, 2011) in the organization of bipolar mitotic spindles (Sueishi et al., 2000; Vanneste et al., 2009; Sturgill and Ohi, 2013). In addition, KIF15 was not identified as a regulator of cell cycle progression in a genome-wide RNAi screen (Neumann et al., 2010). KIF15 is expressed in interphase and shows a remarkably different localization in various cell types – it is localized at centrosomes in HeLa cells (Sueishi et al., 2000), actin bundles in fibroblasts and microtubules in terminally post-mitotic neurons (Buster et al., 2003). GFP-tagged murine KIF15 localized largely to the cytoplasm in HeLa cells, with occasional localization to the plasma membrane, microtubules and punctate structures. A similar localization pattern was observed in lung A549 epithelial carcinoma cells and the normal human fibroblasts BJ-5ta. Furthermore, downregulation of KIF15 induced inhibition of α2 integrin intracellular accumulation in these cells (supplementary material Fig. S3D), indicating that KIF15 plays a role in integrin trafficking in cancer and normal cells. Altered expression levels of KIF15 did not induce apparent alterations in actin or microtubule cytoskeleton and centrosomes, ruling out the

Journal of Cell Science (2014) 127, 2433–2447 doi:10.1242/jcs.137281

possibility that the intracellular accumulation of α2 integrin is altered owing to general cytoskeletal changes (Fig. 4E,F).

Overexpression of GFP-tagged murine KIF15, which is resistant to human siRNAs, partially rescued inhibition of α2 integrin intracellular accumulation caused by KIF15 depletion (Fig. 4A,B). In addition, increased cell-surface α2 integrin expression was measured following KIF15 downregulation (supplementary material Fig. S3C). These data somewhat contradict the directionality of this motor (Boleti et al., 1996). For instance, downregulation of the microtubule plus-end-directed motors KIF1C and KIF16B induced a reduction in the cell-surface localization of α5β1 integrin (Theisen et al., 2012) and transferrin recycling (Hoepfner et al., 2005), respectively. Downregulation of KIF15 induced accumulation of transferrin at the perinuclear region (Fig. 5B), suggesting that it might function in trafficking from the perinuclear recycling compartment. On the contrary, internalization of EGF and transferrin was not influenced by the depletion of KIF15 [Fig. 5B,C,E,F; (Collinet et al., 2010)].

Taken together, our data indicate the possibility that KIF15 might be involved in the surface delivery of an entry factor required for α2 integrin internalization. Indeed, CLASPs are known to specifically regulate β1 integrin internalization (Nishimura and Kaibuchi, 2007; Chao and Kunz, 2009; Ezratty et al., 2005). In agreement with this, we showed that endocytic trafficking of non-clustered α2 integrin might require not only the clathrin-independent but also clathrin-dependent pathways in HeLa cells (Fig. 1F,G). It is known that the FXNPXY-signal-sorting CLASPs (Keyel et al., 2006) Dab2, ARH, and Numb are required for β1 integrin internalization in a number of migrating cells, as well as for the disassembly of focal adhesions (Nishimura and Kaibuchi, 2007; Chao and Kunz, 2009). Our RNAi data using a microscopy-based α2 integrin endocytosis assay largely confirms these observations, with Dab2 being the strongest effector (Fig. 6). Similar to the endocytosis of LDLR (Keyel et al., 2006, Maurer and Cooper, 2006), downregulation of ARH also inhibited the intracellular accumulation of α2 integrin by 40% (Fig. 6B). By contrast, no effect of ARH depletion on the surface expression of β1 integrin was reported (Teckchandani et al., 2009), which might reflect the use of different methodologies. Depletion of Numb, the adaptor with a preference for α5 integrin (Teckchandani et al., 2009), resulted in no significant change in the intracellular accumulation of α2 integrin. As Dab2 is known to inhibit the internalization of unbound β1 integrin (Teckchandani et al., 2009; Teckchandani et al., 2012) and appeared to be the strongest effector of the intracellular accumulation of non-clustered α2 integrin, we focused on Dab2 for further analysis. We could show that the downregulation of KIF15 induced redistribution of punctate Dab2 structures from the plasma membrane (Fig. 7A,C). These are most likely endocytic structures, as they were shown to colocalize with clathrin and AP-2 by >70% in HeLa, NIH3T3 and ES-2 cells (Chetrit et al., 2011; Teckchandani et al., 2009; Morris and Cooper, 2001). In addition, Dab-2-specific structures were shown to colocalize to unbound β1 integrin by >25% (Teckchandani et al., 2009). It is plausible, therefore, that their displacement from the plasma membrane inhibits the internalization of non-clustered α2 integrin. Dab2 is redistributed from the periphery and accumulates at the perinuclear compartment following downregulation of KIF15 (Fig. 7D), but does not colocalize with transferrin under these conditions. In agreement, ce-Dab-1, the *Caenorhabditis elegans* ortholog of Dab2, does not colocalize with Rab11-positive structures (Kamikura and Cooper, 2006). By contrast, the transferrin distribution might be affected by the mislocalized Dab2, which was shown to regulate the recycling of numerous proteins, including transferrin (Fu et al., 2012). As Dab2-mediated internalization of integrins occurs through the clathrin-dependent pathway (Teckchandani et al., 2012; Ezratty et al., 2009; Chao and Kunz, 2009), KIF15 might contribute to the regulation of the endocytic fate of α2 integrin. Whether KIF15 influences Dab2 distribution through direct binding, as demonstrated for the actin-based molecular motor myosin 6 (Spudich et al., 2007; Morris et al., 2002), or indirectly remains to be answered, particularly within the context of cell cycle progression, as Dab2 cell-surface localization and function in endocytosis change throughout the cell cycle (Chetrit et al., 2011). The involvement of KIF15 in clathrin-independent trafficking cannot be ruled out presently, as it was recently demonstrated that kinesins, like KIF13B, enhance cargo recruitment to caveolae (Kanai et al., 2014). The emerging role of KIF15 in the trafficking of α2 integrin, and possibly other cargoes, will be interesting to investigate in a disease context, as KIF15 is overexpressed in various tumours (Bidkhori et al., 2013).

Elucidating the molecular mechanisms influencing the endocytic trafficking of α2β1 integrin, one of the most important collagen receptors, is emerging as an exciting research area. This knowledge is essential for the prevention and treatment of diseases associated with integrin-mediated adhesion. Here, we present a microscopy-based assay that is suitable for high-throughput applications and is helpful in the systematic identification of novel regulators of the intracellular accumulation and/or expression of α2 integrin.

MATERIALS AND METHODS

Cell culture

HeLa cells (ATCC CCL-2) were cultured in MEM (Sigma-Aldrich), A549 cells (ATCC CCL-185) were cultured in F-12K (Sigma-Aldrich), BJ-5ta cells (ATCC CRL-4001) were cultured in a 4:1 mixture of DMEM and Medium 199 (Sigma-Aldrich). All media contained 10% fetal calf serum (FCS), 2 mM glutamine, 100 U/ml penicillin and 100 μg/ml streptomycin. For experiments requiring serum starvation, cells were kept in the respective medium supplemented with 0.01% (w/v) bovine serum albumin (BSA).

Materials

GFP–Rab5, GFP–Rab7a, mCherry–Rab11b and mCherry–Rab4a were a gift from Nathan Brady (DKFZ/BioQuant, Heidelberg University). GFP-MmKIF15 plasmid and anti-KIF15 antibody were a gift from Rene Medema (The Netherlands Cancer Institute). Mouse monoclonal anti-α2-integrin antibody (clone P1E6) was from Merck-Millipore, rabbit monoclonal anti-Dab2 (H-110) and rabbit polyclonal anti-caveolin-1 were from Santa Cruz Biotechnology. Mouse monoclonal anti-Dab2 (clone 52/p96) was from BD Biosciences, mouse monoclonal anti-clathrin and rabbit polyclonal anti-dynamin-2 were from Abcam. Mouse monoclonal anti-α-tubulin (clone DM1A9) was from Cell Signaling Technology, secondary anti-mouse-IgG and anti-rabbit-IgG antibodies coupled to Alexa Fluor 488 and Alexa Fluor 647 were from Invitrogen, anti-rabbit-IgG antibodies coupled to horseradish peroxidase (HRP) were from GE Healthcare and anti-mouse-IgG antibodies coupled to HRP were from R&D. Transferrin–Alexa-Fluor-568, EGF–Alexa-Fluor-555 and phalloidin–Alexa-Fluor-647 conjugates were from Invitrogen. siRNAs targeting Dab2 (SI02780316 and SI02780386), ARH (SI03042634 and SI00111657) and Numb (SI04256994 and SI03199581) were from Qiagen. All other siRNAs are listed in the supplementary material Table S1.

Transfection of siRNAs and cDNAs

For the reverse transfection on cell arrays, 5 μl of 30 μM siRNA was mixed with 3.5 μl of Lipofectamine 2000 (Invitrogen) and 3 μl of

Journal of Cell Science (2014) 127, 2433–2447 doi:10.1242/jcs.137281

Opti-MEM (Invitrogen) containing 0.4 M sucrose and incubated for 20 min at room temperature. Thereafter, it was mixed with 7.25 µl of 0.2% gelatine (w/v) in 0.01% fibronectin (v/v), and used for contact printing with the automated liquid handling robot 'Microlab Star' (Hamilton) on one-chamber Lab-Tek slides (Nunc) using eight solid pins (PTS 600), giving a spot size of ~400 µm diameter. The spot-to-spot distance was set to 1125 µm; thus, a single Lab-Tek chamber fitted 384 spots organized in 12 columns and 32 rows. The whole library of 1084 siRNAs was spotted onto four Lab-Tek chambers, with 6–12 negative control siRNAs distributed randomly across each layout. 5×10^5 cells were seeded per Lab-Tek chamber. Liquid-phase direct transfection with siRNAs or cDNAs in eight-well µ-slides (Ibidi) was performed using Lipofectamine 2000 according to the manufacturer's protocol with 2×10^4 cells seeded per well. Transfection of cells with siRNA and cDNAs was performed 48 h and 24 h before the assay, respectively.

Western blotting

1.5×10^5 HeLa cells were plated in a 12-well plate, transfected with the respective siRNAs and cDNAs, lysed in 80 ml of hot Laemmli buffer, supplemented with 100 mM DTT and separated by 8% SDS-PAGE. The proteins were transferred to polyvinylidene difluoride (PVDF) membrane (Immobilion-P, Merck-Millipore), unspecific proteins were blocked with 5% milk in PBS-Tween, and incubation with the anti-KIF15 and anti-Dab2 antibodies was performed for 1 h at 4℃ or RT, respectively. The proteins of interest were detected by using the ECL system (GE Healthcare). The luminescence was recorded by using the chemiluminescence detection system (Intas) and quantified by using the ImageJ (NIH) 'Analyze Gel' option. The intensity of the relevant band of the blot was expressed as the area of the peak after subtraction of the average background level of the whole blot.

Quantitative RT-PCR and RT-PCR

Preparation of total cellular RNA was performed using TRIzol reagent (Invitrogen) according to the manufacturer's protocol. cDNA was prepared with MMLV reverse transcriptase (Ambion) and oligo-dT primer. Power SYBR Green PCR Mastermix was used for the reaction, which was performed using a StepOnePlus Real-Time PCR system (Applied Biosystems). Relative Dab2, ARH and Numb expression after RNAi was calculated by the $2^{\Delta\Delta CT}$ method using the expression level of GAPDH as a reference for the quantification. Expression of genes of interest in HeLa cells was tested by RT-PCR with up to three sets of primers that were determined by nucleotide BLAST analysis against the human genome and transcriptome. Primers were either designed using Primer BLAST or used as published previously (Jaulin et al., 2007).

Fluorescence-microscopy-based α2 integrin measurements

Cells were serum starved for 14 h, overlaid with 10 µg/ml anti-α2-integrin antibody in MEM-BSA for 1 h on ice, then briefly washed twice with ice-cold MEM-BSA to remove excess antibody and incubated with pre-warmed MEM-BSA at 37℃ to internalize non-clustered α2 integrin. After the internalization, cells were rinsed with PBS, surface-bound antibody was removed with acetic buffer [0.5% (v/v) acetic acid, 0.5 M NaCl, pH 2.6] for 30–40 s, and fixed with 2% paraformaldehyde (PFA) for 20 min at room temperature. Cells were permeabilized with 0.2% (w/v) saponin in 10% (v/v) FCS in PBS and incubated with the secondary antibodies for 1 h at room temperature. When measuring total α2 integrin levels, treatment with the acetic buffer was omitted, cells were permeabilized with 0.2% (w/v) saponin in 10% (v/v) FCS in PBS and stained with the primary and secondary antibodies. α2 integrin on the cell surface was measured by fixing cells with 2% PFA for 20 min at room temperature, quenching with 30 mM glycine for 5 min at room temperature and staining with the primary and secondary antibodies. Clustering by antibody was induced as described previously (Upla et al., 2004) by sequential incubation of cells with the primary anti-α2-integrin and then with secondary antibodies on ice for 1 h each. Then cells were briefly washed twice with ice-cold MEM-BSA and incubated with the pre-warmed MEM-BSA at 37℃ to internalize antibody-clustered α2 integrin. Nuclei were stained with 0.1 µg/ml Hoechst 33342 dye. In order to estimate the efficiency of acid stripping, we compared the average vales of total α2 integrin specific fluorescence, surface-localized α2 integrin and intracellular non-clustered α2 integrin following 60 min of internalization using the same parameters for imaging and image analysis. The highest average fluorescence intensity was obtained for total α2 integrin (100%). The level of non-clustered intracellular α2 integrin obtained after acid stripping was 19.2% and α2 integrin surface-specific fluorescence was 69.5%, together making up to 88.7% of the total α2 integrin fluorescence.

Surface-biotinylation-based α2 integrin internalization assay

The internalization of biotinylated α2 integrin was measured as described previously (Roberts et al., 2001) and the amount of biotinylated α2 integrin was determined by using capture-ELISA.

Quenching-antibody-based β1 integrin internalization assay

The assay was essentially performed as described previously (Arjonen et al., 2012) using anti-CD29 (clone K20) antibodies (Beckman Coulter) conjugated to Alexa Fluor 488 for β1 integrin labeling. After cell fixation, fluorescence intensities were measured by using an EnVision Multilabel Plate Reader (Perkin Elmer).

EGF and transferrin internalization assays

Cells were serum starved for 14 h before the assay, then EGF–Alexa-Fluor-555 was added to MEM-BSA medium to a final concentration of 100 ng/ml and cells were incubated at 37℃ for different lengths of time. Surface attached EGF–Alexa-Fluor-555 was removed with acidic buffer (50 mM glycine, 150 mM NaCl, pH 3.0). For the transferrin endocytic trafficking assay, cells were serum starved for 1 h, then transferrin–Alexa-Fluor-568 was added to MEM-BSA medium to a final concentration of 25 µg/ml. Cells were fixed with 3% PFA for 20 min at room temperature.

Image acquisition by wide-field, confocal and TIRF microscopy

Image acquisition in wide-field mode was performed on an Olympus IX81 ScanR automated inverted microscope (Olympus Biosystems) controlled by ScanR acquisition software. A 10× 0.4 NA air objective (UPlanSApo; Olympus Biosystems) was used for the primary screening on cell arrays and a 20× 0.75 NA air objective (UPlanSApo; Olympus Biosystems) was used for all other experiments. An excitation wavelength of 450–490 nm and emission wavelength of 500–550 nm was used to image α2 integrin, an excitation wavelength of 426–446 nm and emission wavelength of 460–500 nm was used to image EGF–Alexa-Fluor-555, and an excitation wavelength of 545–580 nm and emission wavelength of 610–700 nm was used to image transferrin–Alexa-Fluor-568. An excitation wavelength of 325–375 nm and emission wavelength of 435–475 nm was used to image nuclei in all assays. Confocal imaging was performed on a confocal laser scanning microscope TCS SP5 (Leica Microsystems) using a 63× oil-immersion objective (HCX PL APO 63×/1.4-0.6 Oil CS) and 94-µm diameter pinhole. Laser lines of 488, 561 and 633 nm were used for the excitation of GFP or Alexa Fluor 488, mCherry or Alexa Fluor 568, and Alexa Fluor 647, respectively. TIRF was performed on a Nikon Eclipse Ti TIRF microscope with Nikon Apo TIFR 60× NA 1.49 objective. Laser lines of 488 and 640 nm were used for the excitation of Alexa Fluor 488 and Alexa Fluor 647, respectively.

Colocalization analysis

Colocalization of internalized α2 integrin with overexpressed Rabs in the multi-channelled single confocal plane was performed in ImageJ. The image background was subtracted using a rolling ball algorithm, noise was removed by Gaussian Blur filter and individual structures of >10 pixels in size were binarized and overlapped. In total, peripheral regions of more than five cells/Rab were used for the analysis, with >120 structures analyzed per cell.

Statistical data analysis

During the primary screening, one image completely encompassed an individual spot. Prior to quantification of the internalized integrin-specific

fluorescence intensity, background signal was subtracted by applying a rolling ball algorithm [ScanR Analysis module (Olympus)]. All images were subjected to visual control. The nuclei of individual cells were identified by intensity module, and the regions of nuclei were expanded so as to encompass a maximum area of the cell without touching the neighboring ones. Cell densities were optimized to reach 70–90% confluence to secure clear cell-to-cell separation. As the majority of intracellular α2-integrin-specific fluorescence was clustered in the region of interest, the method allowed unbiased data quantification. For the statistical analysis of the primary screening data, R package (http://cran.r-project.org/) and cellHTS from Bioconductor (http://www.bioconductor.org/) were used. At first, the 2% of cells with the highest integrin-specific fluorescence intensities were excluded for each imaged spot, remaining cell intensities were averaged and B-score normalization (Brideau et al., 2003) was applied to calculate a correction factor for each spot, which would account for spatial effects and between-plate artifacts.

To reliably quantify the intracellular accumulation of α2 integrin, we removed cells with weak endocytic trafficking using a threshold that was set for every experiment separately, according the negative controls, and was kept the same for all samples within the experiment. A Gaussian Mixture Model (Bowman and Azzalini, 1997) was used to automatically cluster the cells into two subpopulations (with high and low efficiencies of α2 integrin intracellular accumulation), assuming that in each subpopulation cells are normally distributed. The median intracellular signal intensities of α2 integrin and cell numbers of each subpopulation was calculated for every spot. Then, the median signal intensity of cells with efficient accumulation was multiplied by the number of such cells and divided by the total cell number in every spot. This ratio was normalized against the median of the negative controls on each cell array. Eventually, the median *z*-score of 5–8 individual replicates of every siRNA was calculated and a one-sided, one-sample Welch's *t*-test was used to compute significance values. A gene was considered as a primary hit when either one out of two tested siRNAs, at least two siRNAs out of six tested or at least three siRNAs out of more than eight siRNAs tested had a consistent inhibitory or acceleratory effect on the intracellular accumulation of α2 integrin. More than 3000 cells were analyzed for every siRNA in the primary screen.

For the validation experiments in eight-chamber μ-slides, 30–42 images/well were taken and analyzed. All other steps of the analysis were the same as in the primary screening, except that a threshold, separating cells with high and low endocytosis, was set manually. For transferrin and EGF trafficking assays all cells in population were taken for the analysis. Statistical significance of difference between experiments throughout this study was tested by Student's two-tailed *t*-test for samples with uneven variance.

Acknowledgements
We thank Rene H. Medema (Netherlands Cancer Institute, Amsterdam, The Netherlands) for the antibodies labeling KIF15 and cDNA encoding KIF15. We thank Reinhard Fässler (MPI, Martinsried, Germany) and Hellyeh Hamidi (Centre of Biotechnology, University of Turku, Finland) for thorough reading of the manuscript and comments.

Competing interests
The authors declare no competing interests.

Author contributions
A.E. and V.S. designed the project and wrote the manuscript; A.E., S.R., A.A. and H.E. performed experiments; B.K. and L.K. performed statistical data evaluation; D.M. and R.R. performed bioinformatics data analysis; R.E., T.L., J.I. and R.P. contributed to the data interpretation.

Funding
This work was supported by Bundesministeriums für Bildung und Forschung; Forschungseinheiten der Systembiologie ViroQuant [grant number 0313923]; European Union FP7 MEHTRICS [grant number HEALTH-F5-2011-278758]; and the Heidelberg University Excellence Cluster CellNetworks [grant number EXC81]. A.E. is supported by the Landesgraduiertenförderung fellowship of Heidelberg University. Deposited in PMC for immediate release.

Supplementary material
Supplementary material available online at
http://jcs.biologists.org/lookup/suppl/doi:10.1242/jcs.137281/-/DC1

References
Arjonen, A., Alanko, J., Veltel, S. and Ivaska, J. (2012). Distinct recycling of active and inactive β1 integrins. *Traffic* **13**, 610-625.
Bass, M. D., Williamson, R. C., Nunan, R. D., Humphries, J. D., Byron, A., Morgan, M. R., Martin, P. and Humphries, M. J. (2011). A syndecan-4 hair trigger initiates wound healing through caveolin- and RhoG-regulated integrin endocytosis. *Dev. Cell* **21**, 681-693.
Bergelson, J. M., Shepley, M. P., Chan, B. M., Hemler, M. E. and Finberg, R. W. (1992). Identification of the integrin VLA-2 as a receptor for echovirus 1. *Science* **255**, 1718-1720.
Bidkhori, G., Narimani, Z., Hosseini Ashtiani, S., Moeini, A., Nowzari-Dalini, A., Masoudi-Nejad, A. (2013). Reconstruction of an integrated genome-scale co-expression network reveals key modules involved in lung adenocarcinoma. *PLoS One* **2013**, 67552.
Boleti, H., Karsenti, E. and Vernos, I. (1996). Xklp2, a novel Xenopus centrosomal kinesin-like protein required for centrosome separation during mitosis. *Cell* **84**, 49-59.
Böttcher, R. T., Stremmel, C., Meves, A., Meyer, H., Widmaier, M., Tseng, H.-Y. and Fässler, R. (2012). Sorting nexin 17 prevents lysosomal degradation of β1 integrins by binding to the β1-integrin tail. *Nat. Cell Biol.* **14**, 584-592.
Bowman, A. W. and Azzalini, A. (1997). *Applied Smoothing Techniques For Data Analysis*. Oxford: Clarendon Press.
Brideau, C., Gunter, B., Pikounis, B. and Liaw, A. (2003). Improved statistical methods for hit selection in high-throughput screening. *J. Biomol. Screen.* **8**, 634-647.
Buster, D. W., Baird, D. H., Yu, W., Solowska, J. M., Chauvière, M., Mazurek, A., Kress, M. and Baas, P. W. (2003). Expression of the mitotic kinesin Kif15 in postmitotic neurons: implications for neuronal migration and development. *J. Neurocytol.* **32**, 79-96.
Carpenter, G. and Cohen, S. (1976). 125I-labeled human epidermal growth factor. Binding, internalization, and degradation in human fibroblasts. *J. Cell Biol.* **71**, 159-171.
Caswell, P. T. and Norman, J. C. (2006). Integrin trafficking and the control of cell migration. *Traffic* **7**, 14-21.
Caswell, P. and Norman, J. (2008). Endocytic transport of integrins during cell migration and invasion. *Trends Cell Biol.* **18**, 257-263.
Caswell, P. T., Spence, H. J., Parsons, M., White, D. P., Clark, K., Cheng, K. W., Mills, G. B., Humphries, M. J., Messent, A. J., Anderson, K. I. et al. (2007). Rab25 associates with alpha5beta1 integrin to promote invasive migration in 3D microenvironments. *Dev. Cell* **13**, 496-510.
Caswell, P. T., Vadrevu, S. and Norman, J. C. (2009). Integrins: masters and slaves of endocytic transport. *Nat. Rev. Mol. Cell Biol.* **10**, 843-853.
Chao, W.-T. and Kunz, J. (2009). Focal adhesion disassembly requires clathrin-dependent endocytosis of integrins. *FEBS Lett.* **583**, 1337-1343.
Chen, J., Diacovo, T. G., Grenache, D. G., Santoro, S. A. and Zutter, M. M. (2002). The alpha(2) integrin subunit-deficient mouse: a multifaceted phenotype including defects of branching morphogenesis and hemostasis. *Am. J. Pathol.* **161**, 337-344.
Chetrit, D., Barzilay, L., Horn, G., Bielik, T., Smorodinsky, N. I. and Ehrlich, M. (2011). Negative regulation of the endocytic adaptor disabled-2 (Dab2) in mitosis. *J. Biol. Chem.* **286**, 5392-5403.
Collinet, C., Stöter, M., Bradshaw, C. R., Samusik, N., Rink, J. C., Kenski, D., Habermann, B., Buchholz, F., Henschel, R., Mueller, M. S. et al. (2010). Systems survey of endocytosis by multiparametric image analysis. *Nature* **464**, 243-249.
D'Souza-Schorey, C. and Chavrier, P. (2006). ARF proteins: roles in membrane traffic and beyond. *Nat. Rev. Mol. Cell Biol.* **7**, 347-358.
Day, P., Riggs, K. A., Hasan, N., Corbin, D., Humphrey, D. and Hu, C. (2011). Syntaxins 3 and 4 mediate vesicular trafficking of α5β1 and α3β1 integrins and cancer cell migration. *Int. J. Oncol.* **39**, 863-871.
de Fougerolles, A. R., Sprague, A. G., Nickerson-Nutter, C. L., Chi-Rosso, G., Rennert, P. D., Gardner, H., Gotwals, P. J., Lobb, R. R. and Koteliansky, V. E. (2000). Regulation of inflammation by collagen-binding integrins alpha1beta1 and alpha2beta1 in models of hypersensitivity and arthritis. *J. Clin. Invest.* **105**, 721-729.
Delevoye, C., Hurbain, I., Tenza, D., Sibarita, J.-B., Uzan-Gafsou, S., Ohno, H., Geerts, W. J. C., Verkleij, A. J., Salamero, J., Marks, M. S. et al. (2009). AP-1 and KIF13A coordinate endosomal sorting and positioning during melanosome biogenesis. *J. Cell Biol.* **187**, 247-264.
Desgrosellier, J. S. and Cheresh, D. A. (2010). Integrins in cancer: biological implications and therapeutic opportunities. *Nat. Rev. Cancer* **10**, 9-22.
Dickson, R. B., Hanover, J. A., Willingham, M. C. and Pastan, I. (1983). Prelysosomal divergence of transferrin and epidermal growth factor during receptor-mediated endocytosis. *Biochemistry* **22**, 5667-5674.
Doherty, G. J. and McMahon, H. T. (2009). Mechanisms of endocytosis. *Annu. Rev. Biochem.* **78**, 857-902.
Donaldson, J. G. and Klausner, R. D. (1994). ARF: a key regulatory switch in membrane traffic and organelle structure. *Curr. Opin. Cell Biol.* **6**, 527-532.
Dozynkiewicz, M. A., Jamieson, N. B., Macpherson, I., Grindlay, J., van den Berghe, P. V., von Thun, A., Morton, J. P., Gourley, C., Timpson, P., Nixon, C.

et al. (2012). Rab25 and CLIC3 collaborate to promote integrin recycling from late endosomes/lysosomes and drive cancer progression. *Dev. Cell* **22**, 131-145.

Eble, J. A. (2005). Collagen-binding integrins as pharmaceutical targets. *Curr. Pharm. Des.* **11**, 867-880.

Eckes, B., Zigrino, P., Kessler, D., Holtkötter, O., Shephard, P., Mauch, C. and Krieg, T. (2000). Fibroblast-matrix interactions in wound healing and fibrosis. *Matrix Biol.* **19**, 325-332.

Emsley, J., Knight, C. G., Farndale, R. W., Barnes, M. J. and Liddington, R. C. (2000). Structural basis of collagen recognition by integrin α2beta1. *Cell* **101**, 47-56.

Erfle, H., Neumann, B., Liebel, U., Rogers, P., Held, M., Walter, T., Ellenberg, J. and Pepperkok, R. (2007). Reverse transfection on cell arrays for high content screening microscopy. *Nat. Protoc.* **2**, 392-399.

Erfle, H., Eskova, A., Reymann, J. and Starkuviene, V. (2011). Cell arrays and high-content screening. *Methods Mol. Biol.* **785**, 277-287.

Ezratty, E. J., Partridge, M. A. and Gundersen, G. G. (2005). Microtubule-induced focal adhesion disassembly is mediated by dynamin and focal adhesion kinase. *Nat. Cell Biol.* **7**, 581-590.

Ezratty, E. J., Bertaux, C., Marcantonio, E. E. and Gundersen, G. G. (2009). Clathrin mediates integrin endocytosis for focal adhesion disassembly in migrating cells. *J. Cell Biol.* **187**, 733-747.

Feire, A. L., Koss, H. and Compton, T. (2004). Cellular integrins function as entry receptors for human cytomegalovirus via a highly conserved disintegrin-like domain. *Proc. Natl. Acad. Sci. USA* **101**, 15470-15475.

Fleming, F. E., Graham, K. L., Takada, Y. and Coulson, B. S. (2011). Determinants of the specificity of rotavirus interactions with the alpha2beta1 integrin. *J. Biol. Chem.* **286**, 6165-6174.

Florian, S. and Mayer, T. U. (2011). Modulated microtubule dynamics enable Hklp2/Kif15 to assemble bipolar spindles. *Cell Cycle* **10**, 3533-3544.

Fu, L., Rab, A., Tang, L. P., Rowe, S. M., Bebok, Z. and Collawn, J. F. (2012). Dab2 is a key regulator of endocytosis and post-endocytic trafficking of the cystic fibrosis transmembrane conductance regulator. *Biochem. J.* **441**, 633-643.

Goshima, G. and Vale, R. D. (2003). The roles of microtubule-based motor proteins in mitosis: comprehensive RNAi analysis in the Drosophila S2 cell line. *J. Cell Biol.* **162**, 1003-1016.

Hansen, C. G. and Nichols, B. J. (2009). Molecular mechanisms of clathrin-independent endocytosis. *J. Cell Sci.* **122**, 1713-1721.

Heino, J., Ignotz, R. A., Hemler, M. E., Crouse, C. and Massagué, J. (1989). Regulation of cell adhesion receptors by transforming growth factor-beta. Concomitant regulation of integrins that share a common beta 1 subunit. *J. Biol. Chem.* **264**, 380-388.

Hemler, M. E., Elices, M. J., Chan, B. M., Zetter, B., Matsuura, N. and Takada, Y. (1990). Multiple ligand binding functions for VLA-2 (alpha 2 beta 1) and VLA-3 (alpha 3 beta 1) in the integrin family. *Cell Differ. Dev.* **32**, 229-238.

Hirokawa, N., Noda, Y., Tanaka, Y. and Niwa, S. (2009). Kinesin superfamily motor proteins and intracellular transport. *Nat. Rev. Mol. Cell Biol.* **10**, 682-696.

Hoepfner, S., Severin, F., Cabezas, A., Habermann, B., Runge, A., Gillooly, D., Stenmark, H. and Zerial, M. (2005). Modulation of receptor recycling and degradation by the endosomal kinesin KIF16B. *Cell* **121**, 437-450.

Huang, C., Lu, C. and Springer, T. A. (1997). Folding of the conserved domain but not of flanking regions in the integrin beta2 subunit requires association with the alpha subunit. *Proc. Natl. Acad. Sci. USA* **94**, 3156-3161.

Humphries, J. D., Byron, A. and Humphries, M. J. (2006). Integrin ligands at a glance. *J. Cell Sci.* **119**, 3901-3903.

Humphries, J. D., Byron, A., Bass, M. D., Craig, S. E., Pinney, J. W., Knight, D. and Humphries, M. J. (2009). Proteomic analysis of integrin-associated complexes identifies RCC2 as a dual regulator of Rac1 and Arf6. *Sci. Signal.* **2**, ra51.

Hynes, R. O. (1992). Integrins: versatility, modulation, and signaling in cell adhesion. *Cell* **69**, 11-25.

Hynes, R. O. (2002). Integrins: bidirectional, allosteric signaling machines. *Cell* **110**, 673-687.

Jaulin, F., Xue, X., Rodriguez-Boulan, E. and Kreitzer, G. (2007). Polarization-dependent selective transport to the apical membrane by KIF5B in MDCK cells. *Dev. Cell* **13**, 511-522.

Kamikura, D. M. and Cooper, J. A. (2006). Clathrin interaction and subcellular localization of Ce-DAB-1, an adaptor for protein secretion in Caenorhabditis elegans. *Traffic* **7**, 324-336.

Kanai, Y., Wang, D. and Hirokawa, N. (2014). KIF13B enhances the endocytosis of LRP1 by recruiting LRP1 to caveolae. *J. Cell Biol.* **204**, 395-408.

Karjalainen, M., Kakkonen, E., Upla, P., Paloranta, H., Kankaanpää, P., Liberali, P., Renkema, G. H., Hyypiä, T., Heino, J. and Marjomäki, V. (2008). A Raft-derived, Pak1-regulated entry participates in alpha2beta1 integrin-dependent sorting to caveosomes. *Mol. Biol. Cell* **19**, 2857-2869.

Keyel, P. A., Mishra, S. K., Roth, R., Heuser, J. E., Watkins, S. C. and Traub, L. M. (2006). A single common portal for clathrin-mediated endocytosis of distinct cargo governed by cargo-selective adaptors. *Mol. Biol. Cell* **17**, 4300-4317.

Kramer, R. H. and Marks, N. (1989). Identification of integrin collagen receptors on human melanoma cells. *J. Biol. Chem.* **264**, 4684-4688.

Krndija, D., Münzberg, C., Maass, U., Hafner, M., Adler, G., Kestler, H. A., Seufferlein, T., Oswald, F. and von Wichert, G. (2012). The phosphatase of regenerating liver 3 (PRL-3) promotes cell migration through Arf-activity-dependent stimulation of integrin α5 recycling. *J. Cell Sci.* **125**, 3883-3892.

Li, W., Cooper, J., Karajannis, M. A. and Giancotti, F. G. (2012). Merlin: a tumour suppressor with functions at the cell cortex and in the nucleus. *EMBO Rep.* **13**, 204-215.

Lobert, V. H., Brech, A., Pedersen, N. M., Wesche, J., Oppelt, A., Malerød, L. and Stenmark, H. (2010). Ubiquitination of alpha 5 beta 1 integrin α2-integrincontrols fibroblast migration through lysosomal degradation of fibronectin-integrin α2-integrincomplexes. *Dev. Cell* **19**, 148-159.

Londrigan, S. L., Graham, K. L., Takada, Y., Halasz, P. and Coulson, B. S. (2003). Monkey rotavirus binding to alpha2beta1 integrin requires the alpha2 I domain and is facilitated by the homologous beta1 subunit. *J. Virol.* **77**, 9486-9501.

Mai, A., Veltel, S., Pellinen, T., Padzik, A., Coffey, E., Marjomäki, V. and Ivaska, J. (2011). Competitive binding of Rab21 and p120RasGAP to integrins regulates receptor traffic and migration. *J. Cell Biol.* **194**, 291-306.

Margadant, C., Monsuur, H. N., Norman, J. C. and Sonnenberg, A. (2011). Mechanisms of integrin activation and trafficking. *Curr. Opin. Cell Biol.* **23**, 607-614.

Margadant, C., Kreft, M., de Groot, D.-J., Norman, J. C. and Sonnenberg, A. (2012). Distinct roles of talin and kindlin in regulating integrin α5β1 function and trafficking. *Curr. Biol.* **22**, 1554-1563.

Matsubara, K., Hinoi, T., Koyama, S. and Kikuchi, A. (1997). The post-translational modifications of Ral and Rac1 are important for the action of Ral-binding protein 1, a putative effector protein of Ral. *FEBS Lett.* **410**, 169-174.

Maurer, M. E. and Cooper, J. A. (2006). The adaptor protein Dab2 sorts LDL receptors into coated pits independently of AP-2 and ARH. *J. Cell Sci.* **119**, 4235-4246.

Mayr, M. I., Hümmer, S., Bormann, J., Grüner, T., Adio, S., Woehlke, G. and Mayer, T. U. (2007). The human kinesin Kif18A is a motile microtubule depolymerase essential for chromosome congression. *Curr. Biol.* **17**, 488-498.

McCartney, B. M. and Fehon, R. G. (1996). Distinct cellular and subcellular patterns of expression imply distinct functions for the Drosophila homologues of moesin and the neurofibromatosis 2 tumor suppressor, merlin. *J. Cell Biol.* **133**, 843-852.

McClatchey, A. I. and Giovannini, M. (2005). Membrane organization and tumorigenesis – the NF2 tumor suppressor, Merlin. *Genes Dev.* **19**, 2265-2277.

Mise-Omata, S., Obata, Y., Iwase, S., Mise, N. and Doi, T. S. (2005). Transient strong reduction of PTEN expression by specific RNAi induces loss of adhesion of the cells. *Biochem. Biophys. Res. Commun.* **328**, 1034-1042.

Morgan, M. R., Hamidi, H., Bass, M. D., Warwood, S., Ballestrem, C. and Humphries, M. J. (2013). Syndecan-4 phosphorylation is a control point for integrin recycling. *Dev. Cell* **24**, 472-485.

Morris, S. M. and Cooper, J. A. (2001). Disabled-2 colocalizes with the LDLR in clathrin-coated pits and interacts with AP-2. *Traffic* **2**, 111-123.

Morris, S. M., Arden, S. D., Roberts, R. C., Kendrick-Jones, J., Cooper, J. A., Luzio, J. P. and Buss, F. (2002). Myosin VI binds to and localises with Dab2, potentially linking receptor-mediated endocytosis and the actin cytoskeleton. *Traffic* **3**, 331-341.

Moser, M., Legate, K. R., Zent, R. and Fässler, R. (2009). The tail of integrins, talin, and kindlins. *Science* **324**, 895-899.

Mosesson, Y., Mills, G. B. and Yarden, Y. (2008). Derailed endocytosis: an emerging feature of cancer. *Nat. Rev. Cancer* **8**, 835-850.

Neumann, B., Walter, T., Hériché, J.-K., Bulkescher, J., Erfle, H., Conrad, C., Rogers, P., Poser, I., Held, M., Liebel, U. et al. (2010). Phenotypic profiling of the human genome by time-lapse microscopy reveals cell division genes. *Nature* **464**, 721-727.

Ning, Y., Buranda, T. and Hudson, L. G. (2007). Activated epidermal growth factor receptor induces integrin alpha2 internalization via caveolae/raft-dependent endocytic pathway. *J. Biol. Chem.* **282**, 6380-6387.

Nishimura, T. and Kaibuchi, K. (2007). Numb controls integrin endocytosis for directional cell migration with aPKC and PAR-3. *Dev. Cell* **13**, 15-28.

Obremski, V. J., Hall, A. M. and Fernandez-Valle, C. (1998). Merlin, the neurofibromatosis type 2 gene product, and beta1 integrin associate in isolated and differentiating Schwann cells. *J. Neurobiol.* **37**, 487-501.

Onodera, Y., Nam, J.-M., Hashimoto, A., Norman, J. C., Shirato, H., Hashimoto, S. and Sabe, H. (2012). Rab5c promotes AMAP1-PRKD2 complex formation to enhance β1 integrin recycling in EGF-induced cancer invasion. *J. Cell Biol.* **197**, 983-996.

Paul, P., van den Hoorn, T., Jongsma, M. L. M., Bakker, M. J., Hengeveld, R., Janssen, L., Cresswell, P., Egan, D. A., van Ham, M., Ten Brinke, A. et al. (2011). A Genome-wide multidimensional RNAi screen reveals pathways controlling MHC class II antigen presentation. *Cell* **145**, 268-283.

Pellinen, T., Arjonen, A., Vuoriluoto, K., Kallio, K., Fransen, J. A. M. and Ivaska, J. (2006). Small GTPase Rab21 regulates cell adhesion and controls endosomal traffic of beta1-integrins. *J. Cell Biol.* **173**, 767-780.

Powelka, A. M., Sun, J., Li, J., Gao, M., Shaw, L. M., Sonnenberg, A. and Hsu, V. W. (2004). Stimulation-dependent recycling of integrin beta1 regulated by ARF6 and Rab11. *Traffic* **5**, 20-36.

Ramirez, N. E., Zhang, Z., Madamanchi, A., Boyd, K. L., O'Rear, L. D., Nashabi, A., Li, Z., Dupont, W. D., Zijlstra, A. and Zutter, M. M. (2011). The $\alpha_2\beta_1$ integrin α2-integrinis a metastasis suppressor in mouse models and human cancer. *J. Clin. Invest.* **121**, 226-237.

Randazzo, P. A., Inoue, H. and Bharti, S. (2007). Arf GAPs as regulators of the actin cytoskeleton. *Biol. Cell* **99**, 583-600.

Rintanen, N., Karjalainen, M., Alanko, J., Paavolainen, L., Mäki, A., Nissinen, L., Lehkonen, M., Kallio, K., Cheng, R. H., Upla, P. et al. (2012). Calpains

promote 〈2β1 integrin α2-integrinturnover in nonrecycling integrin α2-integrinpathway. *Mol. Biol. Cell* **23**, 448-463.

Roberts, M., Barry, S., Woods, A., Van der Sluijs, P. and Norman, J. (2001). PDGF-regulated rab4-dependent recycling of alphavbeta3 integrin α2-integrinfrom early endosomes is necessary for cell adhesion and spreading. *Curr. Biol.* **11**, 1392-1402.

Santoro, S. A. (1999). Platelet surface collagen receptor polymorphisms: variable receptor expression and thrombotic/hemorrhagic risk. *Blood* **93**, 3575-3577.

Shi, F. and Sottile, J. (2008). Caveolin-1-dependent beta1 integrin endocytosis is a critical regulator of fibronectin turnover. *J. Cell Sci.* **121**, 2360-2371.

Shin, S., Wolgamott, L. and Yoon, S.-O. (2012). Integrin trafficking and tumor progression. *Int. J. Cell Biol.* **2012**, 516789.

Simpson, K. J., Selfors, L. M., Bui, J., Reynolds, A., Leake, D., Khvorova, A. and Brugge, J. S. (2008). Identification of genes that regulate epithelial cell migration using an siRNA screening approach. *Nat. Cell Biol.* **10**, 1027-1038.

Simpson, J. C., Joggerst, B., Laketa, V., Verissimo, F., Cetin, C., Erfle, H., Bexiga, M. G., Singan, V. R., Hériché, J.-K., Neumann, B. et al. (2012). Genome-wide RNAi screening identifies human proteins with a regulatory function in the early secretory pathway. *Nat. Cell Biol.* **14**, 764-774.

Skalski, M., Yi, Q., Kean, M. J., Myers, D. W., Williams, K. C., Burtnik, A. and Coppolino, M. G. (2010). Lamellipodium extension and membrane ruffling require different SNARE-mediated trafficking pathways. *BMC Cell Biol.* **11**, 62.

Spudich, G., Chibalina, M. V., Au, J. S., Arden, S. D., Buss, F. and Kendrick-Jones, J. (2007). Myosin VI targeting to clathrin-coated structures and dimerization is mediated by binding to Disabled-2 and PtdIns(4,5)P2. *Nat. Cell Biol.* **9**, 176-183.

Sturgill, E. G. and Ohi, R. (2013). Kinesin-12 differentially affects spindle assembly depending on its microtubule substrate. *Curr. Biol.* **23**, 1280-1290.

Sueishi, M., Takagi, M. and Yoneda, Y. (2000). The forkhead-associated domain of Ki-67 antigen interacts with the novel kinesin-like protein Hklp2. *J. Biol. Chem.* **275**, 28888-28892.

Takada, Y., Ye, X. and Simon, S. (2007). The integrins. *Genome Biol.* **8**, 215.

Tanenbaum, M. E., Macůrek, L., Janssen, A., Geers, E. F., Alvarez-Fernández, M. and Medema, R. H. (2009). Kif15 cooperates with eg5 to promote bipolar spindle assembly. *Curr. Biol.* **19**, 1703-1711.

Teckchandani, A., Toida, N., Goodchild, J., Henderson, C., Watts, J., Wollscheid, B. and Cooper, J. A. (2009). Quantitative proteomics identifies a Dab2/integrin module regulating cell migration. *J. Cell Biol.* **186**, 99-111.

Teckchandani, A., Mulkearns, E. E., Randolph, T. W., Toida, N. and Cooper, J. A. (2012). The clathrin adaptor Dab2 recruits EH domain scaffold proteins to regulate integrin β1 endocytosis. *Mol. Biol. Cell* **23**, 2905-2916.

Theisen, U., Straube, E. and Straube, A. (2012). Directional persistence of migrating cells requires Kif1C-mediated stabilization of trailing adhesions. *Dev. Cell* **23**, 1153-1166.

Tiwari, S., Askari, J. A., Humphries, M. J. and Bulleid, N. J. (2011a). Divalent cations regulate the folding and activation status of integrins during their intracellular trafficking. *J. Cell Sci.* **124**, 1672-1680.

Tiwari, A., Jung, J.-J., Inamdar, S. M., Brown, C. O., Goel, A. and Choudhury, A. (2011b). Endothelial cell migration on fibronectin is regulated by syntaxin 6-mediated alpha5beta1 integrin recycling. *J. Biol. Chem.* **286**, 36749-36761.

Tu, Y., Li, F., Goicoechea, S. and Wu, C. (1999). The LIM-only protein PINCH directly interacts with integrin-linked kinase and is recruited to integrin-rich sites in spreading cells. *Mol. Cell. Biol.* **19**, 2425-2434.

Uematsu, T., Konishi, C., Hoshino, D., Han, X., Tomari, T., Egawa, N., Takada, Y., Isobe, T., Seiki, M. and Koshikawa, N. (2012). Identification of proteins that associate with integrin α2 by proteomic analysis in human fibrosarcoma HT-1080 cells. *J. Cell. Physiol.* **227**, 3072-3079.

Upla, P., Marjomäki, V., Kankaanpää, P., Ivaska, J., Hyypiä, T., Van Der Goot, F. G. and Heino, J. (2004). Clustering induces a lateral redistribution of alpha 2 beta 1 integrin from membrane rafts to caveolae and subsequent protein kinase C-dependent internalization. *Mol. Biol. Cell* **15**, 625-636.

Valdembri, D., Caswell, P. T., Anderson, K. I., Schwarz, J. P., König, I., Astanina, E., Caccavari, F., Norman, J. C., Humphries, M. J., Bussolino, F. et al. (2009). Neuropilin-1/GIPC1 signaling regulates alpha5beta1 integrin traffic and function in endothelial cells. *PLoS Biol.* **7**, e1000025.

Valdembri, D., Sandri, C., Santambrogio, M. and Serini, G. (2011). Regulation of integrins by conformation and traffic: it takes two to tango. *Mol. Biosyst.* **7**, 2539-2546.

Vanneste, D., Takagi, M., Imamoto, N. and Vernos, I. (2009). The role of Hklp2 in the stabilization and maintenance of spindle bipolarity. *Curr. Biol.* **19**, 1712-1717.

Veale, K. J., Offenhäuser, C., Whittaker, S. P., Estrella, R. P. and Murray, R. Z. (2010). Recycling endosome membrane incorporation into the leading edge regulates lamellipodia formation and macrophage migration. *Traffic* **11**, 1370-1379.

Volpicelli-Daley, L. A., Li, Y., Zhang, C.-J. and Kahn, R. A. (2005). Isoform-selective effects of the depletion of ADP-ribosylation factors 1-5 on membrane traffic. *Mol. Biol. Cell* **16**, 4495-4508.

Wang, J. and Howell, K. E. (2000). The luminal domain of TGN38 interacts with integrin beta 1 and is involved in its trafficking. *Traffic* **1**, 713-723.

Winograd-Katz, S. E., Itzkovitz, S., Kam, Z. and Geiger, B. (2009). Multiparametric analysis of focal adhesion formation by RNAi-mediated gene knockdown. *J. Cell Biol.* **186**, 423-436.

Zhang, H., Berg, J. S., Li, Z., Wang, Y., Lång, P., Sousa, A. D., Bhaskar, A., Cheney, R. E. and Strömblad, S. (2004). Myosin-X provides a motor-based link between integrins and the cytoskeleton. *Nat. Cell Biol.* **6**, 523-531.

Zhu, C., Zhao, J., Bibikova, M., Leverson, J. D., Bossy-Wetzel, E., Fan, J.-B., Abraham, R. T. and Jiang, W. (2005a). Functional analysis of human microtubule-based motor proteins, the kinesins and dyneins, in mitosis/cytokinesis using RNA interference. *Mol. Biol. Cell* **16**, 3187-3199.

Zhu, C., Bossy-Wetzel, E. and Jiang, W. (2005b). Recruitment of MKLP1 to the spindle midzone/midbody by INCENP is essential for midbody formation and completion of cytokinesis in human cells. *Biochem. J.* **389**, 373-381.

Zutter, M. M., Sun, H. and Santoro, S. A. (1998). Altered integrin α2-integrinexpression and the malignant phenotype: the contribution of multiple integrated integrin α2-integrinreceptors. *J. Mammary Gland Biol. Neoplasia* **3**, 191-200.